**Journal of Scientific Research & Reports**
**3(10): 1271-1308, 2014; Article no. JSRR.2014.10.001**

**SCIENCEDOMAIN** *international*
www.sciencedomain.org

SCIENCEDOMAIN

# Ferrimagnetic Ordering and Room Temperature Superconductivity in Carbon Nanotubes

**Dmitri Yerchuck*[1], Yauhen Yerchak[2], Vyacheslav Stelmakh[2], Alla Dovlatova[3] and Andrey Alexandrov[3]**

[1] *Heat-Mass Transfer Institute of National Academy of Sciences of RB, Brovka Str.15, Minsk, 220072, RB, Belarus.*
[2] *Belarusian State University, Nezavisimosti Avenue 4, Minsk, 220030, RB, Belarus.*
[3] *M.V.Lomonosov Moscow State University, Moscow, 119899, RF, Russia.*

***Original Research Article***

*Received: 12 August 2013*
*Accepted: 12 December 2013*
*Published: 29 March 2014*

## Abstract

The phenomenon of the formation of uncompensated antiferromagnetic ordering coexisting with the superconductivity at the room temperature in carbon nanotubes, produced by high energy ion beam modification of diamond single crystals in $\langle 100 \rangle$ direction is argued.

*Keywords: Ferrimagnetic Ordering, Nanotubes, Superconductivity*
pacs: 71.10.-w, 73.63.Fg, 78.30.-j, 76.30.-v, 76.50.+g, 78.67.-n

## 1 Introduction and Background

Discovery of new types of superconducting materials has accelerated in 21th century. The commencement of 21th century was commemorated by the discovery of superconductivity, which was observed at relatively high temperature $T_c$ = 40 K in the simple (structurally and electronically) compound $MgB_2$ (1). Its origin is proposed to be arising from charge carriers, which turn out to be placed into very strongly bonding states. They in its turn respond very sensitively to the bond-stretching vibrational modes, see, for instance (2), (3), (4). The boron-boron bonds in the graphite-like layers of $MgB_2$ are rather strong, and it is argument to the appearance of superconductive state. At the same time, the graphite itself and diamond are materials that have more strong bonds (in graphene plane in the case of graphite). Consequently, it allows to consider the carbon and carbon-based materials to be perspective materials for the realization of superconducting states.

Really, the second step in the field was the discovery of superconductivity at 4 K in very heavily boron-doped diamond, reported in 2004 by Ekimov et al (5). Confirmation has been provided by

**Corresponding author: E-mail: dpy@tut.by*

Takano et al, where the value of transition temperature to superconducting state $T_c$ equaled to 7 K in B-doped diamond films (6) was reported.

The origin of the superconductivity in diamond was discussed in a number of theoretical works, see for example (7), (8). In (7), an ab initio study of the superconductivity of boron doped diamond within the framework of a phonon-mediated pairing mechanism was presented. It has been shown in (7), that the role of the dopant, in substitutional position, is unconventional in that, that half of the coupling parameter $\alpha$ originates in strongly localized defect-related vibrational modes, yielding a very peaked Eliashberg function (spectral decomposition of $\alpha$). The electron-phonon coupling potential was found to be extremely large, however $T_c$ remained to be low because of the low value of the density of states at the Fermi level (which is connected with the 3D-nature of the network). The authors of (7) have invited to the study of the case of doped diamond surfaces, where both the contraction of the reconstructed bonds and the 2D-nature of the surface states may lead to much larger $T_c$. We will show, that given idea, concerning of the 2D-nature of carbon states by a preservation of a bond strength (that allows to generate high-frequency phonons) is actually true. The same idea (however in an implicit form) is presented in (8), where the superconductivity of boron-doped diamond is studied in a comparison with its analogy with $MgB_2$.

Authors of (8) conclude, that higher doping should increase $T_c$ somewhat, but effects of three dimensionality primarily on the density of states will keep doped diamond from having a $T_c$ closer to that of $MgB_2$.

Therefore, the authors of above cited works come independently to the same conclusions concerning the nature of superconductivity in heavily boron-doped diamond.

It has to be remarked, that the discovery of superconductivity in diamond followed the discovery of superconductivity in doped silicon clathrates (9) ($T_c$ = 8 K), a cage-like silicon material which crystallizes in the same $sp^3$ environment. Let us also remark, that even though the reported temperatures are rather low by $sp^3$ environment, the superconducting transition of column IV semiconductors is of much interest, since it concerns very common materials, in which column IVa elements in Mendeleev Periodic Table are based elements.

The aforesaid idea to use a 2D-modification of column IVa elements was successfully realized relatively recently (in 2008) in the work (10) and the essential progress in $T_c$ enhancement up to 145 K was achieved. In (10) the transiton to the superconducting state in the silicon sandwich S-Si-QW-S nanostructures prepared by short time diffusion of boron after preliminary oxidation of the n-type Si (100)-surface has been found. The sandwich S-Si-QW-S structures represent themselves the p-type high mobility silicon quantum wells (QW) confined by the nanostructured $\delta$-barriers, heavily doped with boron on the n-type Si (100)-surface. The studies of the cyclotron resonance angular dependences, the scanning tunneling microscopy images and the electron spin resonance (ESR) have shown, that the nanostructured $\delta$-barriers consist of a series of alternating undoped and doped quantum dots, with the doped dots containing the single trigonal ($C_{3v}$-symmetry) dipole centers, $B_+ + B_-$, which are produced by the negative-U reconstruction of the shallow boron acceptors, $2B_0 \rightarrow B_+ + B_-$. The temperature and magnetic field dependencies of the resistance, thermo-emf (Seebeck coefficient), specific heat and magnetic susceptibility were studied and gave the clear evidence of the high temperature superconductivity, $T_c$ = 145 K. It, according to (10), seems to be resulting from the transfer of the small hole bipolarons through the $B_+ + B_-$ dipole centers at the Si-QW-$\delta$-barrier interfaces. The authors consider the coherent tunneling of bipolarons to be the based mechanism of superconductivity.

The next success of the first decade of 21th century in the field of superconductivity studies was the discovery of superconductivity coexisting with antiferromagnetic ordering in the iron-based layered pnictide compound LaFeAsO (that is, also in the material with the prevailed 2D-dimensional strucure). It was repoted approximately in the same time with the discovery of Bagraev et al (in 2008) in (11). Next, the superconductivity has been discovered in both oxygen containing RFeAsO (R = La, Nd, Sm) compounds and in oxygen free $AFe_2As_2$ (A = Ba, Sr, Ca) compounds. It is interesting, that the superconductivity occurs upon doping into the FeAs layers of either electrons or holes. Let

us remark, that owing to the highly two-dimensional structure the pnictides are like to the cuprates. It gave rise to the viewpoint that the physics of the pnictides is similar to the cuprates, and involves insulating behavior. However, there is a growing consensus among researchers that Mott-transition physics does not play a significant role for the iron pnictides, and there are strong indications, that magnetic ordering is of spin-density wave (SDW) type rather than Heisenberg antiferromagnetism of localized spins. In particular, it is evidenced by a relatively small value of the observed magnetic moment per Fe atom, which is around 12-16 percents of $2\mu_B$. In another distinction to the cuprates, electronic structure, which was proposed by band-structure calculations and was supported by angle-resolved photoemission spectroscopy (ARPES), consists of two small hole pockets centered around $\Gamma$ point, $\vec{k} = (0,0)$ and of two small electron pockets centered around M point $\vec{k} = \vec{Q} = (\pi, \pi)$ in the folded Brillouin zone (BZ) (there are two Fe atoms in the unit cell).

Many theoretical studies are devoted at present to the study of the superconductivity state (SSt) formation in pnictides. For instance, the authors of the paper (12) have presented the Fermi-liquid analysis of SDW magnetism and superconductivity in given compounds. They considered a two-band model with small hole and electron pockets located near $\Gamma$ and M points in the folded BZ and argued, that for the geometry indicated, particle-hole and particle-particle channels are nearly identical, and the interactions logarithmically increase at low energies. It has been found, that the interactions in the SDW and extended s-wave ($s^+$ - wave) channels $\vec{k} = (0,0)$, $\vec{k} = \vec{k} + \vec{Q}$ become comparable in a strength being to be the result of the increase in the intraband pair hopping term and the reduction in the Hubbard-type intraband repulsive interaction. The authors also argued, that at zero doping, SDW instability comes first, but at a finite doping, $s^+$ ($s^{\pm}$ in the designation by other authors) superconducting instability occurs at a higher temperature.

$s^+$ pairing bears the similarity to magnetically mediated $d_{x^2-y^2}$ pairing in systems with a large Fermi surface (FS) with an idea that in both cases pairing comes from a repulsive interaction, peaked at $\vec{Q}$, and requires the gap to change its sign under $\vec{k} \to \vec{k} + \vec{Q}$. The difference is that for small pockets, that the gap changes the sign away from the Fermi surface and remains constant along the FS. The spin response of undoped and doped $s^+$ superconductors is analysed in (12) and it has been found that

(i) it possesses a resonance mode which disperses like to Anderson-Bogolyubov mode, that is, with the same velocity,

(ii) intraband scattering by nonmagnetic impurities does not affects the system, but interband scattering affects the system in the same way like to magnetic impurities in a s-wave superconducting state.

Let us touch now on the nature of magnetic ordering in carbon and carbon based materials too. It is well known, that all substances on the whole are magnetics and that classical magnetic ordering is existing in the substances, which are built from the atoms with unfilled inner atomic $d$- or $f$-shells or include given atoms in their elementary units. In other words, magnetically ordered solid substances are the groups of substances, elementary units of which include transition chemical elements with unfilled atomic 3d-, 4d-, 5d-, 6d-shells, or 4f, 5f-shells of rare earth elements. Carbon does not refer to given groups. At the same time, there are at present a number of reports on magnetic ordering in carbon and carbon based materials.

On the experimental discovery of magnetic ordering in carbon structurally ordered systems was reported for the first time during the IBMM-Conference in Knoxville, TN, USA (13) and it was confirmed in the report on E-MRS Conference in Strasbourg, France (14). Let us remark, that the first report almost in the same time on magnetic ordering in structurally non-ordered carbon materials is the work (15), where ferromagnetic ordering in pyrolytic carbon, produced by the chemical vapour deposition method was found. Let us also remark, that simultaneously, the reports (13), (14) were the first reports on the formation by high energy ion beam modification (HEIBM) of diamond single crystals of structurally and magnetically ordered quasi-one-dimensional (quasi-1D) systems along ion tracks, that is, on the formation of new carbon allotropic forms, which was identified with nanotubes (NTs), incorporated in diamond matrix, both like to free NTs with almost cylindrical symmetry and quite

different NTs - with $C_4$ symmetry axis and four petal cross-section figure, which, cannot be ranked with fullerenes. It was shown, that axes of incorporated NTs are very precisely coinciding with ion beam direction (16). The cylindrical symmetry NTs were found to be produced also in polycrystalline diamond films with implantation direction transversely to film surface (17). All new carbon allotropic forms, produced by means of HEIBM possess by a number of very interesting physical properties, reported in (16), (17), (19), (18). When concern the magnetic order, it was established from the study of the temperature dependence of the electron spin resonance absorption intensity, that the incorporated nanotubes, produced by neon HEIBM of a diamond single crystal along $\langle 100 \rangle$ crystallographic direction, possess by weak antiferromagnetic ordering (16), (19), (18), however, copper HEIBM with the implantation direction along $\langle 111 \rangle$ crystal axis, nickel HEIBM with the implantation direction along $\langle 110 \rangle$ axis (16), (19), (18) and boron HEIBM of polycrystalline diamond films with the implantation direction transversely to a film surface (17) lead to the formation of NTs, which possesss by ferromagnetic ordering. It was established directly by the observation of a ferromagnetic spin wave resonance (FMSWR) (17), (19), (18). It was found, that magnetic ordering is an inherent property for given carbon electronic systems and it is not connected with magnetic impurities, since starting samples were selected in that way, that the absolute spin number of paramagnetic impurities and the other paramagnetic structural imperfections in the samples studied did not exceed the value $\sim 10^{12}$ spins. Let us remark, that antiferroelectric ordering has been found recently (20) in the same pure carbon allotropic form - quasi-1D carbon zigzag-shaped nanotubes (CZSNTs), obtained by boron- and copper-HEIBM of diamond single crystals in the $\langle 111 \rangle$-direction. It was established by means of the detection of the new optical phenomenon - the antiferroelectric spin wave resonance (AFESWR). The given phenomenon was theoretically described and experinmentally confirmed for the first time by infrared (IR) spectroscopy studies of carbynoids and polyvinilidenhalogenides in (21). Let us indicate on some significant conclusions, which were done on the base of foregoing results. The results obtained mean, that pure carbon systems in the form of quasi-1D CZSNTs and in the form of 1D-carbon chains are multiferroic systems. In its turn, the experimental observation of a multiferroicity in quasi-1D CZSNTs and carbynoids means the breakdown of a space inversion symmetry along CZSNT hypercomplex (that is, along a $n$-dimensional symmetry axis $z$, see for details (22), (20), where $n$ is the number of the chains in CZSNT) and along a carbon chain symmetry axis in carbynoids. In the case of CZSNTs, it agrees well with the model of quasi-1D CZSNTs (22), (20), based on a bond dimerization in all chain components of quasi-1D CZSNT along its hypercomplex symmetry axis $z$. Really, the bond dimerization leads actually to an inversion symmetry breakdown along $z$, confirming additionally the model itself. At the same time it is clear, that the inversion symmetry breakdown is the necessary condition for the appearance of a nonzero polarisation by atomic displacements, that is, for the appearance of an antiferroelecricity (however it seems to be not the sufficient condition in the general case).

Qualitatively, the appearance of magnetic ordering in carbon systems was explained in (23). It is indicated in (23) that the key for the explanation of the appearance of magnetic ordering in carbon systems and in the other systems based on IVb-group elements of Periodic Mendeleev Table - Si, Ge - is concealed in the atomic structure of IVb-group elements, more specifically, the crucial moment is the fact, that free C, Si, and Ge atoms have the spin value S = 1 and the orbital moment value L = 1, at that, the spin and orbital moments have opposite directions, resulting in the strict compensation of each other. It is clear, that in condensed matter, that is, in some carbon allotropic forms or in C-based or Si-, Ge-based compounds the compensation of spin and orbital moments of individual atoms can be destroyed. It can be achieved, for example, by the change of orbital or spin moment directions relatively each other. The second possibility is the change of the value, for instance, of orbital moments of individual C, Si, or Ge atoms. It is concluded in (23) that the C-, Si-, Ge-based magnetic materials can be elaborated with magnetic properties to be comparable with those ones, which possess the materials, produced on the base of transition chemical elements with unfilled atomic 3d-, 4d-, 5d-, 6d-shells, or 4f-, 5f-shells of rare earth elements. Moreover, magnetic properties of given magnetic materials are predicted to be regulable.

The mechanisms to achieve the given goal can be very different. One of the mechanisms is discussed in (23).

The aim of given work is to study in more details the properties of non-cylindrical nanotubes, produced in diamond single crystals by high energy ion implantation, which are possessing instead of $C_\infty$ symmetry axis the only by $C_4$ symmetry axis and to establish the mechanisms of the formation of magnetic and electric ordering in given NTs. They seems to be the appropriate candidates for high temperature superconducting systems, since both the mechanisms of superconductivity like to those ones established in $MgB_2$ and in pnictides, briefly reviewed above, can be realized (see Section IV). Moreover, it will be theoretically shown, that the usual s-wave mechanism, proposed by Bardeen, Cooper, Schrieffer (BCS) (25) can also be realized. In other words, the multicannel superconductivity is predicted in given NTs.

Let us accentuate once again, that the given systems - corrugated cylindrical nanotubes, incorporated in diamond single crystals, are representing the quite new class of carbon structures, and they cannot be considered to be limit case of the fullerene series (whereas it takes place for cylindrical nanotubes), since they have the alternating-sign curvature of the four-petal NT-surface in the direction, being to be transversal to the NT-axis (the curvature of cylindrical nanotubes like to fullerenes is not sign-alternating).

# 2 Experimental Technique

Samples of type IIa natural diamond, implanted by high energy ions of nickel (the energy of ions in ion beam was $335\ MeV$) have been studied. Paramagnetically pure samples have been selected so that the absolute spin number did not exceed the value $\approx 10^{12}$ spins in each of the samples used before implantation. Ion implantation was performed along the $\langle 100 \rangle$ crystal direction (ion beam dose was $5 \times 10^{13}\ cm^{-2}$) transversely to sample (100)-plane and uniformly along all the plane surface. The temperature of the samples during the implantation was controlled and it did not exceed 400 K. ESR spectra were registered on X-band ESR-spectrometer "Radiopan" at room temperature by using of $TE_{102}$ mode rectangular cavity. The ruby standard sample was permanently placed in the cavity on its sidewall. One of the lines of ESR absorption by $Cr^{3+}$ point paramagnetic centers (PC) in ruby was used for the correct relative intensity measurements of ESR absorption, for the calibration of the amplitude value of magnetic component of the microwave field and for precise phase tuning of the modulation field. The correct relative intensity measurements become to be possible owing to unsaturating behavior of ESR absorption in ruby in the range of the microwave power applied, which was $\approx 100$ mW in the absence of an attenuation. Unsaturable character of the absorption in a ruby standard was confirmed by means of the measurements of the absorption intensities in two identical ruby samples in dependence on the microwave power level. The first sample was standard sample, permanently placed in the cavity, the second sample was placed in the cavity away from the loop of the magnetic component of the microwave field so, that its resonance line intensity was about 0.1 of the intensity of the corresponding line of the first sample. Both the samples were registered simultaneously but their absorption lines were not overlapped owing to slightly different sample orientations. The foregoing intensity ratio was precisely preserved for all microwave power values in the range used, which indicates, that really ruby samples are good standard samples in ESR-spectroscopy studies.

# 3 Results

The ESR spectra observed in carbon nanotubes, produced by nickel high energy $\langle 100 \rangle$ ion beam modification of natural diamond single crystals, are presented in Figures 1 to 3 in crystal directions [100], [111] and 60 degrees from [100] correspondingly. The line in the range (1865 - 1981) G

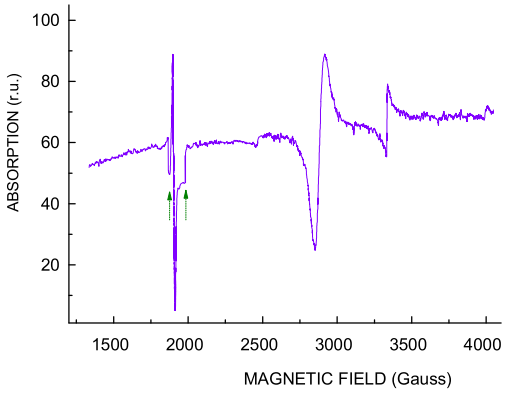


Figure 1: Spectral distribution of ESR absorption intensity in diamond single crystal, implanted by high energy nickel ions by beam direction transversely (100) sample plane, the sample was rotated in (0$\bar{1}$1) plane, $\vec{H_0}||$ [100] crystal axis, leftmost line belongs to ruby standard

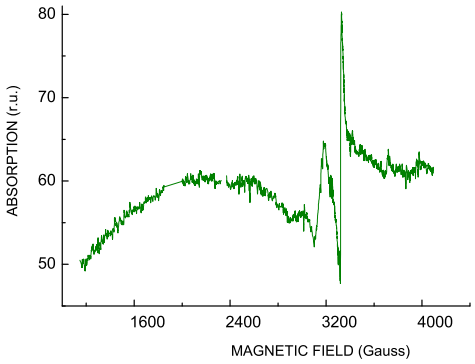


Figure 2: Spectral distribution of ESR absorption intensity in diamond single crystal, implanted by high energy nickel ions by beam direction transversely (100) sample plane, the sample was rotated in (0$\bar{1}$1) plane, $\vec{H_0}||$ [111] crystal axis

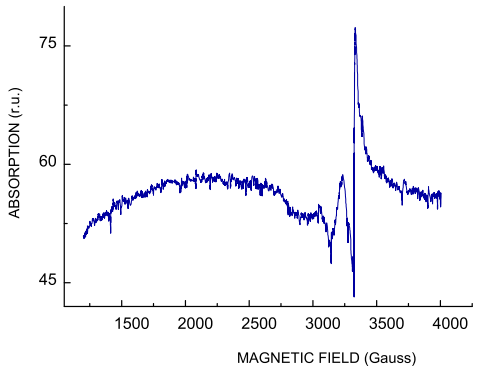


Figure 3: Spectral distribution of ESR absorption intensity in diamond single crystal, implanted by high energy nickel ions by beam direction transversely (100) sample plane, the sample was rotated in $(0\bar{1}1)$ plane, the angle between $\vec{H}_0$ and [100] crystal axis is 60 degrees

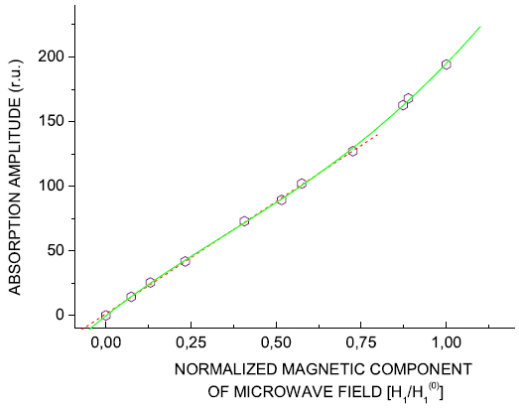


Figure 4: Dependence of absorption amplitude of the left line L in ESR spectrum of NTs incorporated in diamond single crystal on magnetic component of microwave field at $\vec{H}_0||$[100] crystal axis

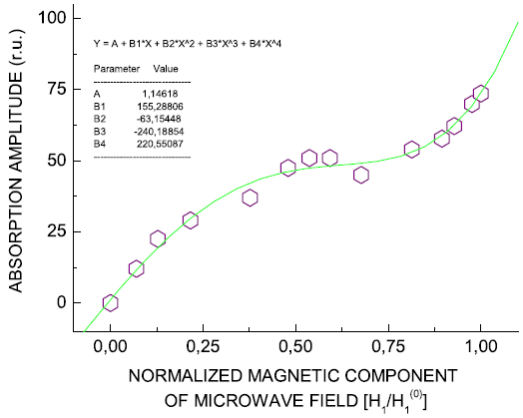


Figure 5: Dependence of absorption amplitude of the right broad line $R_b$ in ESR spectrum of NTs incorporated in diamond single crystal on magnetic component of microwave field at $\vec{H_0}||$ [100] crystal axis

(given field range is indicated by arrows in Figure 1) is the absorption line by ruby standard, it is shifted to botton in Figure 1 and it is removed in the same range in Figures 2 and 3. The most intensive two lines in the range (3000 - 3500) G were excited spontaneously the only by very precise orientation of external static magnetic field $\vec{H}_0$ in the plane coinciding with the plane, transversal to the implantation plane and containing the implantation direction. Therefore, resulting spectrum in the range (3000 - 3500) G was consisting of three lines, at that both two new lines have rather large anisotropic linewidths. Let us designate given lines by $R_b$ for the right broad line and by L for the left line. The right broad line was overlapped with relatively narrow almost isotropic line, designated by $R_n$ (given line was observed by usual sample orientation). Additionally, very broad strongly intensive anisotropic absorption lines were observed. They represent themselves two backgrounds with two dip positions (in integrated spectrum) at $\sim 2410$ G and $\sim 2892$ G by the spectrum registration in the direction corresponding to [111] diamond lattice direction, Figure 2. Dip positions for given background absorption were coinciding by static magnetic field direction in 60 degrees from [100] diamond crystal direction, Figure 3. It seems to be the display of the fact, that the symmetry of the interaction, leading to the appearance of a very strong background absorption is determined by an inherent symmetry of NTs, produced by [100] HEIBM, which is not connected with a potential effect of the diamond lattice presence.

Dependencies of absorption amplitudes of L-line and $R_b$-line on magnetic component of microwave field at the fixed orientation of polarising magnetic field $\vec{H_0}||$[100] crystal axis have been studied, Figures 4 and 5. It is seen from the comparison of the Figures 4 and 5, that given dependencies are quite different. The dependence, presented for L-line in Figure 4, is superlinear. It is similar to the dependencies, which were earlier observed in the samples, modified by HEIBM with copper, neon, nickel ions (however with dose $5 \times 10^{14}$ (16), (19), (18), that is, in the case of an entire modification of the diamond layer, which is localised near the implantation surface). It means, that the layer was consisting then the only of NTs, which seem to be interacting with each other. In the studied sample (integral dose is $5 \times 10^{13}$), individual NTs are isolated by the diamond structure, nevertheless the superlinear dependence is taking place, which seems to be unexpected. Let us remark, that the initial part of the curve, presented in Figure 4, can in the principle be approximated by a linear dependence (dashed line), although it is clear from the comparison with the approximation of the whole curve (solid line in Figure 4), that even the initial part, strongly speaking, is not linear. Solid line in Figure

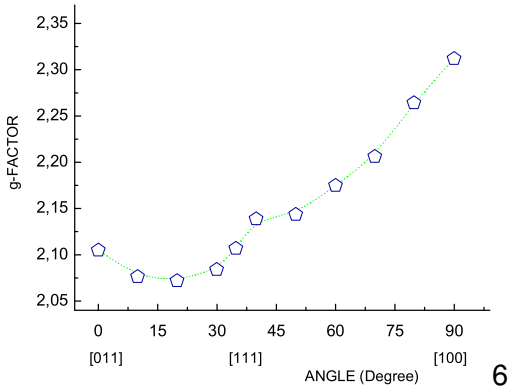


6

Figure 6: Angular dependence of g-factor of the left line L in ESR spectrum of NTs incorporated in diamond single crystal, the sample was rotated in $(0\bar{1}1)$ plane

4 is the polinomial fit with the function $f(x) = b_0 + b_1x + b_2x^2 + b_3x^3 + b_4x^4$, where $b_0 = -0.17117$, $b_1 = 208.92305$, $b_2 = -139.06624$, $b_3 = 159.14424$, $b_4 = -33.90983$.

It is seen, that the dependence of the absorption amplitude of the right broad line $R_b$ in the ESR spectrum of NTs on the magnetic component of the microwave field is strongly nonlinear. It is characterised for the values of the relative magnetic component of the microwave field $H_1/H_1^{(0)}$ in the range (0-0.75) by the usual saturating law, but in the range (0.75-1) it acquires the prominent superlinear nonsaturating character. The dependence for an ESR absorption kinetics in the form, presented in Figure 5, is observed in ESR-spectroscopy for the first time. It can be approximated by the solid line, which represents itself the polynomial fit in accordance with the relation $Y(x) = A + B_1x + B_2x^2 + B_3x^3 + B_4x^4$, where $A = 1.14618$, $B_1 = 0.77956$, $B_2 = -0.00159$, $B_3 = -3.03868e^{-5}$, $B_4 = 1.40072e^{-7}$.The angular dependence of g-factor of the left line L in the ESR spectrum of NTs in the sample studied is presented in Figure 6. It consist of two branches. One branch is in the angle range 0-50 degrees from [100] crystal lattice direction, that is, in the direction, which is coinciding with NT axis direction in limits of the experimental inaccuracy by implantation providing (not exceeding 1 degree), the second branch is in the angle range 50-90 degrees. Let us remark, that the connection point of two branches, equaled to 50 degrees for g-values of L-line is not coinciding with the point of the junction of two dips in the very broad (and consequently very intensive) absorption, testifying on the existence of two different resonance processes, which are responsible for the appearance of L-line and very broad lines. The deviation of g-values from free electron value g = 2.0023 is very large, at that, the minimal value is achieved in the range 16-20 degrees from the [011] direction in diamond lattice and it is equal to $\approx 2.0719$, maximal g-value corresponds to the NT-axis direction, that is, to [100] crystal lattice direction and it is equal to $\approx 2.3120$. The given values are characteristic for the systems with strong magnetic ordering. Consequently, we have obtained the direct proof of the spontaneous transition of NT system, incorporated in diamond lattice, in the state with the strong magnetic ordering in ESR conditions. The angular dependence of ESR absorption intensity of the left line L has qualitatively opposite character to its g-factor dependence. The maximal absorption value corresponds to the direction, being to be transversal to NT axis, which is coincides with [011] direction in a diamond lattice, Figure 7. The additional maximum is observed at 60 degrees from the given direction. Let us remark, that both the maxima in the angular dependence of ESR absorption intensity of the line L are observed also in the angular dependence of its linewidth, Figure 8, indicating, that the main features in the angular dependence of ESR absorption intensity are governed by the angular dependence of the linewidth. It is confirmed also by that, that the very pronounced local maximum is observed in the angular dependence of the absorption amplitude of the line L in the range

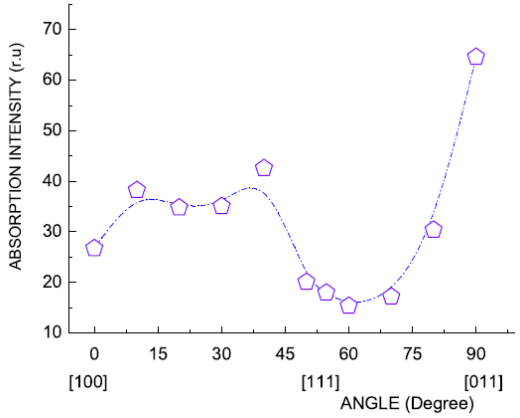


Figure 7: Angular dependence of ESR absorption intensity of the left line L in ESR spectrum of NTs incorporated in diamond single crystal, the sample was rotated in $(0\bar{1}1)$ plane

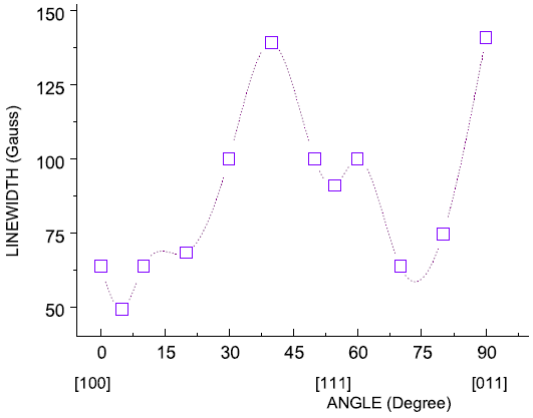


Figure 8: Angular dependence of linewidth of the left line L in ESR spectrum of NTs incorporated in diamond single crystal, the sample was rotated in $(0\bar{1}1)$ plane

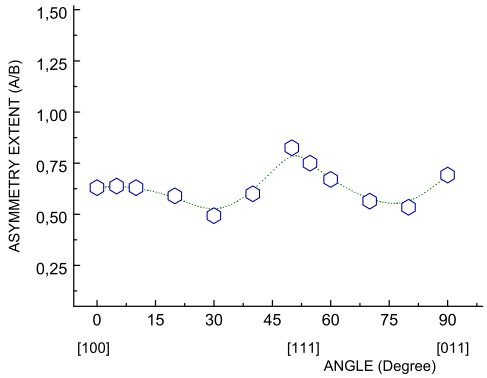


Figure 9: Angular dependence of asymmetry extent A/B of the left line L in ESR spectrum of NTs incorporated in diamond single crystal, the sample was rotated in $(0\bar{1}1)$ plane

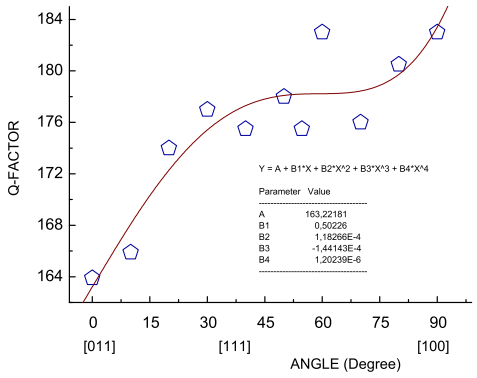


Figure 10: Angular dependence of the cavity Q-factor with the sample implanted by high energy nickel ions by beam direction transversely (100) sample plane, the sample was rotated in $(0\bar{1}1)$ plane

10-20 degrees from [100] crystal lattice direction (the corresponding Figure is not presented). At the same time it is not pronounced in the angular dependence of the absorption intensity, see Figure 7. It is seen from the angular dependence of the linewidth of the line L, Figure 8, that its value is strongly dependent on the direction of the static magnetic field applied. There are four local maxima, main maximum is achieved at [011] direction with the linewidth value, which is equal to 140.9 G, very pronounced maximum is observed at the angle in 40 degrees from [100] lattice direction, the linewidth value is equal to 139.1 G, that is, it is comparable with the main maximum value. Two, not very pronounced maxima are observed correspondingly at at the angle between 10 and 20 degrees and at the angle in 60 degrees from [100] lattice direction, the linewidth values are equal correspondingly to 68.7 G and 100 G. The main minimum is achieved near the NT axes' direction, more stricly, at $\approx$ 5 degrees from the given direction with the linewidth value, which is equal to 49.1 G. The foregoing linewidth values are characteristic for the states with strong magnetic ordering, that is, it is additional argument in favour of the conclusion on the formation of strong magnetic ordering in the sample studied. It is also seen from Figure 8, that two branches of the linewidth growth, starting at $\approx$ 5 degrees and in the range 70-75 degrees from [100] direction, have the resemblance. That seems to be the indication on the same origin of the linewidth broadening process, determining the foregoing growth branches. It is also significant, that linewidth anisotropy value, equaled tp 91.8 G is very large, indicating on the appearance of very strong mechanism of line broadening by the spontaneous transition of the NT-system studied in the state with the ESR spectra above described.

Especially interesting, that the line L is asymmetric, Figure 9. However, the angular dependence of the ratio $A/B$ of the asymmetry extent is disagreeding with the angular dependence, which has to be observed by an usual Dyson effect in metals or semiconductors (26). The value $B/A$ is equal 2.55 for static (immobile) paramagnetic centers (PC) in conductive media in the case of thick samples (in a comparison with the scin depth) and it is determined by the space dispersion contribution (27), which is appeared in conductive media by the microwave field propagation into the conductive sample. It corresponds to the ratio of the space dispersion contribution and the absorption contribution to the resulting ESR response, equaled to (1 : 1) (27) in in the case of thick samples. The value $B/A$ for the absorption derivative is increasing from 2.55 to more than 19 for mobile PCs (or by the presence of a spin diffusion) in the dependence on the velocity of mobile PCs (or on the rate of the spin diffusion) (28). In the case of thin samples, the ratio $B/A$ has intermediate values, between 1 and above indicated, depending on the thickness of the samples. It is seen from Figure 9, that the ratio A/B is anisotropic. The maximal A/B value (correspondingly, minimal $B/A$) is near [111] crystal lattice direction and it is equal to 0.83, Figure 9. The minimal A/B (maximal $B/A$) value is near 60 degrees from [011] crystal lattice direction and it is equal to 0.49, Figure 9. Let us remark, that by an usual Dyson effect in conducting thin samples (in particular, in the samples with metallic NTs, producing the network) the maximal deviation from the ratio A/B = 1 has to be observed by the microwave field propagation direction along the sample side with the maximal size of the implanted region in the rotation plane, that is by $H_0$ along [100] crystal direction, in the case, when the network is opaque for the microwave field in the direction, transverse to NT axis direction, or by $H_0$ along [011] in the case, when the network is opaque the only for the microwave field propagation in the direction, coinciding with NT axes. [It is taken into account, that the propagation direction is transverse to the static magnetic field direction]. The observed maximal deviation of the ratio A/B from A/B = 1 at $\approx 60$ degrees from [011] confirms the conclusion on the nontrivial nature of an Dyson-like effect in the sample studied.

The presence of the ruby standard allowed to control the cavity $Q$-factor, Figure 10. It seems to be substantial, that $Q$-factor is increasing in the ranges, where the deviation of the ratio A/B from A/B = 1 is also increasing, that is, the increase is starting near 60 degrees from [011] crystal lattice direction and the increase takes place in the range near 10-30 degrees from the same [011] crystal direction, compare Figures 10 and 9. For an usual Dyson effect it has to be conversely, $Q$-factor has to be minimal in the direction of the maximal deviation of ratio A/B from A/B = 1, that is, near 30 degrees from [100] crystal lattice direction, Figure 9. It is seen from Figure 10, that $Q$-factor has in

the given direction the maximal value. We have to remark, thatwhich indicates simultaneously, that the approximating solid line does not run over the point, corresponding to the maximal Q-value. It means, that the approximation has to be more accurate (more of experimental points is required).

# 4 Discussion

It will be further argued, that the results above described are agreed with the spontaneous transition of the system to the state, which characterises by the coexistence simultaneously of antiferromagnetic (AFM) uncompensated ordering and the superconductivity, which is realized in electron spin resonance conditions and it is not appearing without the resonance. Given specific conditions seem to be indicating, that the origin of the given state, that is mechanisms, leading to its formation cannot be entirely coinciding with known ones, including above reviewed. To solve given task, it seems to be necessary to know the nature of charge and spin carriers and the mechanisms of a carrier transport and interactions of charge and spin carriers both between themselves and with phonons and photons in NTs studied. There seems to be paramount significant the same task for nanoelectronics, spintronics and for the other branches of nanotechnology.

Let us remark, that in the theory of 1D electronic systems, in particular, in the theory of conducting NTs is existing the following concept. It is based on the work of Tomonaga (29) and on the work of Luttinger (30), from which follows, that the electron-electron interaction destroys the sharp Fermi surface and leads to a breakdown of the Landau Fermi liquid (LFL) theory for 1D systems. The resulting non-LFL state is commonly called Luttinger liquid (LL), or sometimes Tomonaga-Luttinger liquid (TLL). The term "Luttinger liquid" has been coined by Haldane (31). The given approach was used upto now for the description of the universal low-energy properties of all 1D conductors. The theory of LL (TLL) predicts the pronounced power-law suppression of the transport current and the density of states, and the effect of a spin-charge separation. The nature of the spin and charge carriers accorging to LL (TLL) theory is the following. They are chargeless spin 1/2 quasiparticles - spinons and spinless quasiparticles with the charge $\pm$ e - holons. The universality of LL (TLL) description means that the physical properties of 1D systems have to be not depending on details of the model, of the interaction potential, and so on. They are only characterized by a few parameters - critical exponents. Moreover, the LL (TLL) concept is believed to be valid for arbitrary statistical properties of the particles, that both for fermions and bosons. It is also interesting that along with a paradigm for non-Fermi liquid physics for the description of any 1D systems the concept of LL (TLL) was extended for the description of 2D and 3D correlated electrons in systems with a linear dispersion law (32).

Concerning NTs, let us remark, that the single-wall carbon nanotubes (SWCNTs) are considered in many works to be 1D objects (it is not always correct, especially for standard NTs with adiameter in several nanometers and more), which can be described the only within the frames of LL (TLL) concept. Moreover, SWCNTs are considered to be the best model systems for the LL (TLL) state demonstration. The arguments used to confirm the given conclusion are the following. It is the experimental observation of a power-law behavior by measuring the tunneling conductance of SWNTs in dependence on temperature and voltage. It has to be remarked however, that power laws are widely spread in the physics. They can approximate some other dependences or can follow from the other theories too. Electron force microscopic measurements showed also the ballistic nature of a transport in conducting SWNTs, predicted by the LL (TLL) model. Ballistic behavior of transpot phenomena can also be determined by the other causes, not connected with LL (TLL) model, see, for instance, (33), (34). An insufficiency of the substantiation of the applicability of LL (TLL) model to SWCNTs becomes to be evident, if to take into account, that the main feature of the given model - a spin-charge separation by the spinon-holon mechanism has not been observed.

It has to be also taken into account, that both the models LL (TLL) and LFL are the oversimplified models, since they do not take into account the nonlinearity of the fermion spectrum on the one hand

and the presence of electron-phonon interactions on the other hand. In fact both the models describe not strongly adequately the real processes, since the changes in the charge state of an arbitrary atom in 1D chain, being to be the result of the electron-electron interaction, are always accompanied by the changes in the phonon subsystem (and vice versa). It is the consequence of generic coupling between operators of a creation and an annihilation in the electron subsystem and in the phonon field (see futher for more details). Let us also remember, that the key argument for the insertion of the notion "Luttinger liquid" itself (31) is in fact also based on the simplification, determined by a linearization of the generic spectrum of particles in the neighborhood of Fermi points in k-space. At the same time, the divergencies arising in the perturbation theory in 1D-case are the consequence just of the given simplification. From here it is not follows, that 1D Fermi liquid description is incorrect in the general case, which takes into account the electron-phonon interaction and/or the nonlinearity of the generic spectrum of particles in a neighborhood of Fermi points in k-space.

So we come to the conclusion, that the description of NTs within the frames of LL concept seems to be also the oversimplification. To correct the given situation, let us consider the new model of quantum liquid. It was developed in (35) where the concept of the description of 1D correlated electronic systems wihtin the framework of 1D Fermi liquid (FL) was restored.

It was considered in (35) the concept of 1D FL on the example of well known 1D system - *trans*-polyacetylene (t-PL). It is in fact the generalization of well known model of conjugated organic 1D conductors proposed by Su, Schrieffer, Heeger (SSH-model) (36), (37), which is formally a Fermi gas model. It will be futher shown that SSH-model takes the intermediate position between Fermi gas and Fermi liquid models, since it takes into consideration the electron-electron correlations in implicit form. The further generalization, for instance, for the application of 1D FL model immediately to the quasi-1D carbon zigzag shaped nanotubes can be obtained by using of the hypercomplex number theory like to the works (22), (20), where the hypercomplex number theory was applied for the interpretation of quantum optics effects in the carbon zigzag shaped NTs.

Let us represent for the convenience of the readers the main moments of the calculation and the results of the work (35).

The Born-Oppenheimer approximation was considered and starting Hamiltonian was the following

$$\hat{\mathcal{H}}(u) = \hat{\mathcal{H}}_0(u) + \hat{\mathcal{H}}_{\pi,t}(u) + \hat{\mathcal{H}}_{\pi,u}(u). \tag{4.1}$$

The first term in (4.1) is

$$\hat{\mathcal{H}}_0(u) = \sum_m \sum_s (\frac{\hat{P}_m^2}{2M^*}\hat{a}_{m,s}^+\hat{a}_{m,s} + Ku_m^2\hat{a}_{m,s}^+\hat{a}_{m,s}). \tag{4.2}$$

It represents itself the sum of the operator of the kinetic energy of CH-groups' motions (the first term in (4.2)) and the operator of the $\sigma$-bonding energy (the second term). Coefficient $K$ in (4.2) is effective $\sigma$-bonds spring constant, $M^*$ is total mass of CH-group, $u_m$ is configuration coordinate for $m$-th CH-group, which corresponds to the translation of $m$-th CH-group along the symmetry axis $z$ of the chain, $m = \overline{1,N}$, $N$ is a number of CH-groups in the chain, $\hat{P}_m$ is the operator of the impulse, conjugated to the configuration coordinate $u_m$, $m = \overline{1,N}$, $\hat{a}_{m,s}^+$, $\hat{a}_{m,s}$ are creation and annihilation operators of a creation or an annihilation of a quasiparticle with the spin projection $s$ on the $m$-th chain site in $\sigma$-subsystem of t-PA. The second term in (4.1) can be represented in the form of two components and it is

$$\begin{aligned}\hat{\mathcal{H}}_{\pi,t}(u) = \hat{\mathcal{H}}_{\pi,t_0}(u) + \hat{\mathcal{H}}_{\pi,t,\alpha_1}(u) = \sum_m \sum_s [(t_0(\hat{c}_{m+1,s}^+\hat{c}_{m,s} + \hat{c}_{m,s}^+\hat{c}_{m+1,s}) + \\ (-1)^m 2\alpha_1 u(\hat{c}_{m+1,s}^+\hat{c}_{m,s} + \hat{c}_{m,s}^+\hat{c}_{m+1,s})],\end{aligned} \tag{4.3}$$

where $\hat{c}_{m,s}^+$, $\hat{c}_{m,s}$ are creation and annihilation operators of a creation or an annihilation of a quasiparticle with the spin projection $s$ on the $m$-th chain site in $\pi$-subsystem of t-PA. It is the resonance interaction

(the hopping interaction in a tight-binding model approximation) of quasiparticles in $\pi$-subsystem of t-PA electronic system, which is considered to be Fermi liquid, and in which the only constant and linear terms in the Taylor series expansion of the resonance integral about the dimerized state are taking into account.

The operator $\hat{\mathcal{H}}(u)$ is invariant under spatial translations with period $2a$, where $a$ is the projection of spacing between two adjacent CH-groups in the undimerized lattice on the chain axis direction, which is equal to 1.22 $\mathring{A}$. It means, that all various wave vectors $\vec{k}$ in $\vec{k}$-space will be in the reduced zone with the module of $\vec{k}$ in the range $-\frac{\pi}{2a} \leq k \leq \frac{\pi}{2a}$ (37). The reduced zone is considered like to usual semiconductors to be consisting of two subzones - conduction $(c)$ band and valence $(v)$ band. Then the operators $\{\hat{c}^{+}_{m,s}\}$, $\{\hat{c}_{m,s}\}$, $m = \overline{1,N}$, were represented in (35) in the form

$$\begin{aligned} \{\hat{c}_{m,s}\} &= \{\hat{c}^{(c)}_{m,s}\} + \{\hat{c}^{(v)}_{m,s}\}, \\ \{\hat{c}^{+}_{m,s}\} &= \{\hat{c}^{+(c)}_{m,s}\} + \{\hat{c}^{+(v)}_{m,s}\}, \end{aligned} \tag{4.4}$$

related to $\pi - c$- and $\pi - v$-band correspondingly, and $\vec{k}$-space operators were defined

$$\begin{aligned} \{\hat{c}^{(c)}_{k,s}\} &= \{\frac{i}{\sqrt{N}} \sum_{m} \sum_{s} (-1)^{m+1} \exp(-ikma) \hat{c}^{(c)}_{m,s}\}, \\ \{\hat{c}^{(v)}_{k,s}\} &= \{\frac{1}{\sqrt{N}} \sum_{m} \sum_{s} \exp(-ikma) \hat{c}^{(v)}_{m,s}\}, \end{aligned} \tag{4.5}$$

$m = \overline{1,N}$.

The $\sigma$-operators $\{\hat{a}^{+}_{m,s}\}$ and $\{\hat{a}_{m,s}\}$, $m = \overline{1,N}$ were also represented in the form like to (4.4) for $\pi$-operators and transforms, analogous to (4.5), were defined. It leads to the following expression for the operator $\hat{\mathcal{H}}_0(u)$

$$\hat{\mathcal{H}}_0(u) = \sum_{k} \sum_{s} (\frac{\hat{P}^2}{2M^*} + Ku^2)(\hat{n}^{\sigma,c}_{k,s} + \hat{n}^{\sigma,v}_{k,s}), \tag{4.6}$$

where $\hat{n}^{\sigma,c}_{k,s}$ and $\hat{n}^{\sigma,v}_{k,s}$ are operators of number of $\sigma$-quasiparticles in $\sigma$-$c$-band and $\sigma$-$v$-band correspondingly.

The independence of $|u_m|$ on $m$, $m = \overline{1,N}$, was taken into consideration.

The expression for $\hat{\mathcal{H}}_{\pi,t_0}(u)$ in terms of $\{\hat{c}^{(c)}_{k,s}\}$ and $\{\hat{c}^{(v)}_{k,s}\}$ is coinciding with known corresponding expression in (36), (37) and it is

$$\hat{\mathcal{H}}_{\pi,t_0}(u) = \sum_{k} \sum_{s} 2t_0 \cos ka (\hat{c}^{+(c)}_{k,s} \hat{c}^{(c)}_{k,s} - \hat{c}^{+(v)}_{k,s} \hat{c}^{(v)}_{k,s}) \tag{4.7}$$

The expression for the second part of operator $\hat{\mathcal{H}}_{\pi,t}(u)$ in terms of $\{\hat{c}^{(c)}_{k,s}\}$ and $\{\hat{c}^{(v)}_{k,s}\}$ is also coinciding in its form with known corresponding expression in (36), (37) and it is given by

$$\hat{\mathcal{H}}_{\pi,t,\alpha_1}(u) = \sum_{k} \sum_{s} 4\alpha_1 u \sin ka (\hat{c}^{+(v)}_{k,s} \hat{c}^{(c)}_{k,s} + \hat{c}^{+(c)}_{k,s} \hat{c}^{(v)}_{k,s}), \tag{4.8}$$

where the subscript $\alpha_1$ in the Hamiltonian designation indicates on the taking into account the part of electron-phonon interaction, connected with resonance interaction (hopping) processes. The expression for the operator $\hat{\mathcal{H}}_{\pi,u}(u)$, which describes the part of electron-phonon interaction, determined by an interaction between quasiparticles in a Fermi liquid state of $\pi$-subsystem in terms of $\{\hat{c}^{(c)}_{k,s}\}$ and $\{\hat{c}^{(v)}_{k,s}\}$ is the following

$$\hat{\mathcal{H}}_{\pi,u,\alpha_2}(u) = \sum_{k} \sum_{k'} \sum_{s} \alpha_2(k,k',s) \hat{c}^{+(c)}_{k',s} \hat{c}^{+(v)}_{k',s} \hat{c}^{(v)}_{k,s} \hat{c}^{(c)}_{k,s}. \tag{4.9}$$

The contribution of the term, corresponding the only to the interaction between the quasiparticles in different bands, which seems to be the most essential, was considered. The expression for $\alpha_2(k,k',s)$ was obtained in the form

$$\begin{aligned}&\alpha_2(k,k',s) = b|v_{0v}|^2|v_{0c}|^2V_{0(c)}uV_{0(v)}|\phi_{0cs}|^2|\phi_{0vs}|^2\times\\&\frac{N}{2\pi(q_l-q_j)(q_r-q_n)}Re\{\exp[i(k_lm_l-k_jm_j)a]\exp ika\}\times\\&Re\{\exp[i(k'_rm_r-k'_nm_n)a]\exp ik'a\},\end{aligned} \tag{4.10}$$

where $|\phi_{0cs}|^2$, $|\phi_{0vs}|^2$ are squares of the modules of the wave functions $|k_{j,s}\rangle$ and $|k'_{j,s}\rangle$ respectively, $k = k_{ph}(q_l - q_j)$, $k' = k'_{ph}(q_r - q_n)$, $q_l, q_j, q_r, q_n \in N$ with additional conditions $(q_l - q_j)a \le L$, $(q_r - q_n)a \le L$, $b$ - is the aspect ratio, which in principle can be determined by a comparison with an experiment. Here the values $(q_l - q_j)$, $(q_r - q_n)$ determine the steps in a pairwise interaction with the phonon participation and they are considered to be fixed. The processes, for which $k = k'$, are considered. Consequently, $(q_r - q_n)$ = $(q_l - q_j)$ and the operator $\hat{\mathcal{H}}_{\pi,u,\alpha_2}(u)$ is

$$\hat{\mathcal{H}}_{\pi,u,\alpha_2}(u) = \sum_k\sum_{k'}\sum_s 4\alpha_2(s)u\sin ka\sin k'a\hat{c}^{+(c)}_{k',s}\hat{c}^{+(v)}_{k',s}\hat{c}^{(v)}_{k,s}\hat{c}^{(c)}_{k,s}, \tag{4.11}$$

where $\alpha_2(s)$ is

$$\alpha_2(s) = \frac{b}{4}|v_{0v}|^2|v_{0c}|^2V_{0(c)}V_{0(v)}|\phi_{0cs}|^2|\phi_{0vs}|^2\times\frac{N}{2\pi[(q_l-q_j)]^2} \tag{4.12}$$

The system of operators $\hat{c}^{+(c)}_{k',s}$, $\hat{c}^{+(v)}_{k',s}$, $\hat{c}^{(v)}_{k,s}$, $\hat{c}^{(c)}_{k,s}$ corresponds to noninteracting quasiparticles, and it is understandable, that in the case of interacting quasiparticles their linear combination has to be used

$$\begin{bmatrix}\hat{a}^{(v)}_{k,s}\\ \hat{a}^{(c)}_{k,s}\end{bmatrix} = \begin{bmatrix}\alpha_{k,s} & -\beta_{k,s}\\ \beta_{k,s} & \alpha_{k,s}\end{bmatrix}\begin{bmatrix}\hat{c}^{(v)}_{k,s}\\ \hat{c}^{(c)}_{k,s}\end{bmatrix}, \tag{4.13}$$

Then it has been shown, that the diagonal part of Hamiltonian $\hat{\mathcal{H}}_{\pi,t,\alpha_1}(u)$, which corresponds to SSH one-electron treatment of electron-phonon coupling, can be represented in the form

$$\hat{\mathcal{H}}^d_{\pi,t,\alpha_1}(u) = \sum_k\sum_s 2\Delta_k\alpha_{k,s}\beta_{k,s}(\hat{n}^{(c)}_{k,s} - \hat{n}^{(v)}_{k,s}), \tag{4.14}$$

where $\Delta_k = 4\alpha_1 u\sin ka$, $\hat{n}^{(c)}_{k,s}$ is the density of the operator of the quasiparticles' number in $c$-band, $\hat{n}^{(v)}_{k,s}$ is the density of the operator of the quasiparticles' number in $v$-band.

The diagonal part $\hat{\mathcal{H}}^d_{\pi,u,\alpha_2}(u)$ of the operator $\hat{\mathcal{H}}_{\pi,u,\alpha_2}(u)$ of the pairwise interaction, which is linear in the displacement coordinate $u$ and leads to the participation of the phonons, is given by the expression

$$\begin{aligned}&\hat{\mathcal{H}}^d_{\pi,u,\alpha_2}(u) = 4\alpha_2 u\sum_k\sum_{k'}\sum_s\alpha_{k'}\beta_{k'}(\hat{n}^{(v)}_{k',s} - \hat{n}^{(c)}_{k',s})\\&\times\alpha_{k,s}\beta_{k,s}(\hat{n}^{(v)}_{k,s} - \hat{n}^{(c)}_{k,s})\sin k'a\sin ka\end{aligned} \tag{4.15}$$

Let us remark, that the Hamiltonian $\hat{\mathcal{H}}_{\pi,u,\alpha_2}(u)$ describes the attraction between the electrons, it can lead to the formation of Cooper pairs in a $\pi$-subsystem and to the superconductivity of both of an usual $s$-wave type, described in (24), (25), that is, with Cooper pairs in singlet S = 0 state and with Cooper pairs in triplet S = 1 state. It is like to well-known possibility of the formation of singlet and triplet excitons and it seems to be the substantial conclusion being to be the key moment for

the coexistence of a superconductivity and magnetic ordering. In fact, the new mechanism for a superconductivity was proposed.

The diagonal part $\hat{\mathcal{H}}^{d}_{\pi,t_0}(u)$ of the operator $\hat{\mathcal{H}}_{\pi,t_0}(u)$ in terms of operator variables $\hat{a}^{(c)}_{k,s}$ $\hat{a}^{(v)}_{k,s}$ is given by the relation

$$\hat{\mathcal{H}}^{d}_{\pi,t_0}(u) = \sum_k \sum_s \epsilon_k(\alpha^2_{k,s} - \beta^2_{k,s})(\hat{n}^{(c)}_{k,s} - \hat{n}^{(v)}_{k,s}), \tag{4.16}$$

where $\epsilon_k = 2t_0 \cos ka$.

The operator transformation for the $\sigma$-subsystem, analogous to (4.13) shows, that the Hamiltonian $\hat{\mathcal{H}}_0(u)$ is invariant under the given transformation, that is, it can be represented in the form, given by (4.6).

To find the values of the elements of the matrix in the relation (4.13), the Hamiltonian $\hat{\mathcal{H}}(u)$ has been tested for the conditional extremum in the dependence on the variables $\alpha_k$, $\beta_k$ with the condition $\alpha^2_{k,s} + \beta^2_{k,s} = 1$.

Two values for the energy of quasiparticles, indicating on the possibility of the formation of the quasiparticles of two kinds both in $c$-band and $v$-band have been obtained. They are the following

$$\begin{aligned} E^{(c)}_k(u) &= \frac{\mathcal{Q}^2\Delta^2_k - \epsilon^2_k}{\sqrt{\epsilon^2_k + \mathcal{Q}^2\Delta^2_k}}, \\ E^{(v)}_k(u) &= \frac{\epsilon^2_k - \mathcal{Q}^2\Delta^2_k}{\sqrt{\epsilon^2_k + \mathcal{Q}^2\Delta^2_k}} \end{aligned} \tag{4.17}$$

and

$$\begin{aligned} E^{(c)}_k(u) &= \sqrt{\epsilon^2_k + \mathcal{Q}^2\Delta^2_k}, \\ E^{(v)}_k(u) &= -\sqrt{\epsilon^2_k + \mathcal{Q}^2\Delta^2_k} \end{aligned} \tag{4.18}$$

The factor $\mathcal{Q}$ is determined by the relation

$$[1 + \frac{\alpha_2}{2\alpha_1} \sum_k \sum_s \frac{\mathcal{Q}\Delta_k \sin ka}{\sqrt{\epsilon^2_k + \mathcal{Q}^2\Delta^2_k}}(n^{(c)}_{k,s} - n^{(v)}_{k,s})] = \mathcal{Q}, \tag{4.19}$$

where $n^{(c)}_{k,s}$ is the eigenvalue of the density operator of the quasiparticles' number in $c$-band, $n^{(v)}_{k,s}$ is the eigenvalue of the density operator of the quasiparticles' number in $v$-band. The quasiparticles with the energy, determined by (4.18) at $\mathcal{Q} = 1$ are the same quasiparticles, that were obtained in known SSH-model.

Sufficient conditions for the minimum of the functions $E(\alpha_{k,s}\beta_{k,s})$ were obtained by a standard way, which was used also in (20). It consist in that, that the second differential of the energy being to be the function of three variables $\alpha_{k,s}$, $\beta_{k,s}$ and $\lambda_{k,s}$ has to be a positively defined quadratic form. From the condition of a positiveness of three principal minors of the quadratic form coefficients the three sufficient conditions for the energy minimum have been obtained. Their analysis has showed, that SSH-like solution is inapplicable for the description of standard processes, passing near an equilibrium state by any parameters (35). The quasiparticles, described by SSH-like solution, can be created the only in a strongly nonequilibrium state with the inverse population of the levels in $c$- and $v$-bands. At the same time, the solution, the energy of quasiparticles for which is determined by (4.17), can be realised both in a near equilibrium and in a strongly non-equilibrium state of $\pi$-subsystem of t-PA, which is considered to be the quantum Fermi liquid (35).

The continuum limit for the ground state energy of the $t$-PA chain with SSH-like quasiparticles will coincide with known solution (37), if to replace $\Delta_k\mathcal{Q} \to \Delta_k$. The calculation of the ground state

energy $E_0^{[u]}(u)$ of the $t$-PA chain with quasiparticles' branch, which is stable near an equilibrium by taking into account, that in a ground state $n_{k,s}^c = 0$, $n_{k,s}^v = 1$, in the continuum limit gives

$$E_0^{[u]}(u) = -\frac{2Na}{\pi}\int\limits_0^{\frac{\pi}{2a}} \frac{(\mathcal{Q}\Delta_k)^2 - \epsilon_k^2}{\sqrt{\mathcal{Q}\Delta_k)^2 + \epsilon_k^2}} dk + 2NKu^2. \tag{4.20}$$

Then, the calculation of the integral results in the expression

$$E_0^{[u]}(u) = \frac{4Nt_0}{\pi}\{F(\frac{\pi}{2}, 1-z^2) + \frac{1+z^2}{1-z^2}[E(\frac{\pi}{2}, 1-z^2) - F(\frac{\pi}{2}, 1-z^2)]\} + 2NKu^2, \tag{4.21}$$

where $z^2 = \frac{2\mathcal{Q}\alpha_1 u}{t_0}$, $F(\frac{\pi}{2}, 1-z^2)$ is the complete elliptic integral of the first kind and $E(\frac{\pi}{2}, 1-z^2)$ is the complete elliptic integral of the second kind. The approximation of the ground state energy at $z \ll 1$ for the quasiparticles , being to be stable nearby a equilibrium gives

$$E_0^{[u]}(u) = N\{\frac{4t_0}{\pi} - \frac{6}{\pi}\ln\frac{2t_0}{\mathcal{Q}\alpha_1 u}\frac{4(\mathcal{Q}\alpha_1)^2u^2}{t_0} + \frac{28(\mathcal{Q}\alpha_1)^2u^2}{\pi t_0} + ...\} + 2NKu^2. \tag{4.22}$$

It is seen from (4.22), that the energy of quasiparticles, described by the given solution, has the form of Coleman-Weinberg potential with two minima at the values of the dimerization coordinate $u_0$ and $-u_0$ like to the energy of quasiparticles, described by SSH-solution. It is understandable, that further considerations, including the electrically neutral S = 1/2 soliton and electrically charged spinless soliton formation, that is, the appearance of the phenomenon of the spin-charge separation, by the FL description of 1D systems will be coinciding in its mathematical form with those ones in SSH-model.

Thus, in (35) was established the possibility to describe the physical properties of 1D systems within the frames of 1D quantum FL including the mechanism of the appearance of the most prominent feature of 1D systems - the phenomenon of the spin-charge separation. It was also found the possibility of the simultaneous formation of the superconducting state and the state with magnetic ordering in 1D FL.

Let us remark, that the model proposed takes into consideration the electron-electron correlations in the explicit form, which seems to be ground for its application to electronic systems of quasi-1D NTs, where electron-electron correlations are known to be rather strong. In particular, it can be used for an analysis of ESR spectra. It can be done by above indicated manner, that is by using of a hypercomplex number theory analogously to the theoretical analysis of quantum optics effects in (22) and the analysis in (20) of Raman spectra in quasi-1D NTs. It is essential, that the FL soliton spin-charge separation mechanism in quasi-1D carbon NTs has the experimental confirmation (16), (19), (18), whereas the LL (FLL) spin-charge separation mechanism has not been found. It seems to be the direct confirmation of the applicability of the theory of FL above considered to carbon quasi-1D NTs. Given results mean, that the explanation of the results, presented in Section III, has to take into consideration the FL behavior of an electronic system of NTs, incorporated in a diamond single crystal in [100] direction. It is the main conclusion from the given theory for the subsequent analysis of the experimental results presented. On the other hand, it justifies the brief representation of the results of the work (35).

The results above considered show, that the shape of $\pi$-solitons (or $\sigma$-solitons) is given by the expression with the same mathematical form both in SSH-model and in its FL generalization. It is

$$|\phi(n)|^2 = \frac{1}{\xi_{\pi(\sigma)}} sech^2[\frac{(n-n_0)a}{\xi_{\pi(\sigma)}} - v_{\pi(\sigma)}t]\cos^2\frac{n\pi}{2}, \tag{4.23}$$

where $n, n_0$ are, correspondingly, variable and fixed numbers of $CH$-units in $CH$-chain, $a$ is $C-C$ interatomic spacing projection on the chain direction, $v_{\pi(\sigma)}$ is $\pi$ ($\sigma$)-soliton velocity, $t$ is the time, $\xi_{\pi(\sigma)}$ is $\pi(\sigma)$ coherence length. It is seen, that $\pi$-solitons ($\sigma$-solitons) differ in fact the only by a numerical

value of the coherence length in SSH-model and in its FL generalization. Really, the coherence lengths $\xi_{0\pi}$ and $\xi_{0\sigma}$ are determined by the relation (38)

$$\xi_{0\pi} = \frac{\hbar v_F}{\Delta_{0\pi}}, \xi_{0\sigma} = \frac{\hbar v_F}{\Delta_{0\sigma}}, \tag{4.24}$$

where $\Delta_{0\sigma}$, $\Delta_{0\pi}$ are $\sigma-$ and $\pi$-bandgap values at $T = 0K$, $v_F$ is the Fermi velocity. In SSH-model $v_F$ is proportional to $t_0$, in SSH-FL-model, here presented, $v_F$ is proportional to the sum $t_0 + t_1$. It allows to explain some discrepancy between the theoretical value in SSH-model and experimental values for $\xi_\pi$ and its dispersion, depending on a production technology. The theoretical value in SSH-model for $\xi_\pi$ in t-PA is $7a$, and it is low boundary in the range $7a - 11a$, obtained for $\xi_\pi$ from experiments (39). It means, that in the samples with the $\pi$-soliton coherence length, equaled to $11a$, $t_1$ is equal to $0.57t_0$ at the same t-PA band gap value (it is possible, since factor $Q$ is independent on $t_1$ and can be close to 1).

Consequently, we come to the conclusion, that the constant component in Taylor expansion of the electron-electron interaction potential with the term, proportional to $t_1$, is substantial and that the value of $t_1$ can depend on the preparation technology.

Above described experimental results obtained by ESR study of NTs, formed in diamond single crystals in the result of the $\langle 100 \rangle$ ion beam modification indicate, that for the correct description of NTs' properties the $\sigma$-electronic subsystem has to be taken into consideration. It follows immediately from the appearance of inherent magnetic symmetry directions, which are not coinciding with host lattice symmetry directions. From the other hand, the analysis of numerical values of g-factor and linewidth values, Figure 6, Figure 8, means, that magnetic interactions are strong and their strength values are comparable with the corresponding values in usual magnetic systems with unfilled inner shells. At the same time, it is shown in (23), that in the case, when magnetic ordering is determined the only by $\pi$-subsystem of the NTs, the magnetic interactions are relatively weak, magnetic ordering symmetry characteristics are governed by symmetry directions of surrounding diamond lattice (with an accuracy of a some possible deviation of a implantation direction from a selected diamond lattice axis symmetry direction, which however is not exceeding 1 degree above indicated). It takes place in NTs produced by means of $\langle 110 \rangle$ ion beam modification and $\langle 111 \rangle$ ion beam modification. It seems to be evident, that by $\langle 100 \rangle$ ion beam modification we have the case of strong antiferromagnetic (AFM) ordering. Really, the conclusion on just AFM ordering (but not ferromagnetic) is in agreement with observation of two both very broad and two moderately broad lines. The appearance of two AFM-resonance lines (if a linearly polarised microwave field is used by the detection, that was the case in our experiments) was established by Kittel in the work (40), which was the first work on the theory of a AFM-resonance. It has been found in the related our work (41), that magnetic moments of two sublattices being to be opposite directed are uncompensated in their magnitude, that is, strongly speaking, we are dealing with an uncompensated AFM-resonance or, in other words, with a ferrimagnetic resonance. This is so indeed, since the ratio of intensities of the absorption, corresponding to L and $R_b$-lines is equal to $\approx 3.5$ (41).

Let us consider the following Hamiltonian

$$\hat{\mathcal{H}}(u) = \hat{\mathcal{H}}_0(u) + \hat{\mathcal{H}}_1(u) + \hat{\mathcal{H}}_2(u) + \hat{\mathcal{H}}_3(u) + \hat{\mathcal{H}}_4(u), \tag{4.25}$$

where $u$ is the configuration coordinate along the symmetry axis $z$ of the individual chain of NT. It is suggested to be independent on a site position and on a subsystem kind. The operator $\hat{\mathcal{H}}_0(u)$ is

$$\hat{\mathcal{H}}_0(u) = \sum_{\vec{k}} \sum_{m} \sum_{q} \sum_{s} \varepsilon^{mq}(u) \hat{c}^{+}_{\vec{k}ms} \hat{c}_{\vec{k}qs}, \tag{4.26}$$

in which subscripts $m, q = \{\pi, \sigma\}$, $s$ is the spin projection, $\vec{k}$ is the wave vector, $\hat{c}^{+}_{\vec{k}ms}$, $\hat{c}_{\vec{k}ms}$ are operators of the creation and the annihilation of the quasiparticle with the spin projection $s$ and with the wave vector $\vec{k}$ in $m$th ($q$th) subsystem, $\varepsilon^{mq}(u)$ are the resonance interaction integrals (describing the hopping interaction in a tight-binding model approximation) of quasiparticles in $\pi$-subsystem of

electronic system, in $\sigma$-subsystem of electronic system, which are considered to be 1D quantum Fermi liquids, and between $\pi$- and $\sigma$-subsystems.

The operator $\hat{\mathcal{H}}_1$ is

$$\hat{\mathcal{H}}_1(u) = \sum_m \sum_j U_1(j,m,u)\hat{c}^+_{jms(\uparrow)}\hat{c}_{jms(\uparrow)}\hat{c}^+_{jms(\downarrow)}\hat{c}_{jms(\downarrow)}, \tag{4.27}$$

where $j = \overline{1,N}$ is the site position, $U_1(j,m,u)$ is the intrasubsystem Coulomb coupling parameter, which is dependent in the general case on $j,m,u$. The operator $\hat{\mathcal{H}}_2(u)$ is

$$\hat{\mathcal{H}}_2(u) = \sum_{m>q} \sum_j U_2(j,m,q,u) \sum_s \hat{c}^+_{jms}\hat{c}_{jms} \sum_s \hat{c}^+_{jqs}\hat{c}_{jqs} \tag{4.28}$$

where $U_2(j,m,q,u)$ is the intersubsystem Coulomb coupling parameter, which is dependent in the general case on $j,m,q,u$. The operator $\hat{\mathcal{H}}_3(u)$ is

$$\hat{\mathcal{H}}_3(u) = \sum_{m>q} \sum_j \sum_s \sum_{s'} J_1(j,m,q,u)\hat{c}^+_{jms}\hat{c}^+_{jqs'}\hat{c}_{jms'}\hat{c}_{jqs}, \tag{4.29}$$

where $J_1(j,m,q,u)$ is the inter-subsystem Hund rule coupling, which is dependent in the general case on $j,m,q,u$. The operator $\hat{\mathcal{H}}_4(u)$ is

$$\hat{\mathcal{H}}_4 = \sum_{m\neq q} \sum_j J_2(j,m,q,u)\hat{c}^+_{jms(\uparrow)}\hat{c}^+_{jms(\downarrow)}\hat{c}_{jqs(\downarrow)}\hat{c}_{jqs(\uparrow)} \tag{4.30}$$

where $J_2(j,m,q,u)$ is the pair hopping parameter, which is dependent in the general case on $j,m,q,u$.

Like to the foregoing consideration the Hamiltonians $\hat{\mathcal{H}}_1(u)$ and $\hat{\mathcal{H}}_2(u)$ can be expanded in Taylor series about the dimerized state. So, restricting by two first terms in Taylor expansion, we have

$$\hat{\mathcal{H}}_1(u) = \sum_m \sum_j (U_1^{(0)} + (-1)^j 2\alpha_1^m u)\hat{c}^+_{jms(\uparrow)}\hat{c}_{jms(\uparrow)}\hat{c}^+_{jms(\downarrow)}\hat{c}_{jms(\downarrow)}, \tag{4.31}$$

where $\{\alpha_1^m\}$, $m = \{\pi,\sigma\}$ are constants of electron-phonon interactions, accompanying the processes of intrasubsystem Coulomb interations.

$$\hat{\mathcal{H}}_2(u) = \sum_{m>q} \sum_j (U_2^{(0)} + (-1)^j 2\alpha_2^{mq} u) \sum_s \hat{c}^+_{jms}\hat{c}_{jms} \sum_s \hat{c}^+_{jqs}\hat{c}_{jqs}, \tag{4.32}$$

where $\{\alpha_2^{mq}\}$, $m,q = \{\pi,\sigma\}$ are constants of electron-phonon interactions, accompanying the processes of intersubsystem Coulomb interactions. It is clear, that the second terms in (4.31) and in (4.32) describe the attraction between strongly correlated electrons, it can explain the nature of the pairing mechanism in our samples and in high temperature superconductors at all.

The Hamiltonian $\hat{\mathcal{H}}(u)$ can be considered to be the basic Hamiltonian for its generalization to describe the properties of carbon NTs, produced by $\langle 100\rangle$ ion beam modification of diamond single crystals, in particular, for the analysis of ESR data above described. The generalization of the Hamiltonian $\hat{\mathcal{H}}(u)$ can be done by the way, proposed in (22) on the basis of hypercomplex number theory, at that, it has to be taken into account, that, strongly speaking, NTs, produced by $\langle 100\rangle$ implantation can be described within the framework of hypercomplex number theory by its generalization too, since $C_4$ symmetry indicates on inequivalence of the chains along the NT hypercomplex axis.

Let us remark, that the Hamiltonian (4.25) is similar to two-orbital-Hamiltonian, proposed in (42) for the spectral analysis of the iron-based superconductors. It will be almost coinciding in the case when $\{\alpha_1^m\} = 0$, $m = \{\pi,\sigma\}$, $\{\alpha_2^{mq}\} = 0$, $m,q = \{\pi,\sigma\}$, and when $J_1(j,m,q,u)$, $J_2(j,m,q,u)$ are independent on $j,m,q,u$. The difference in the given case consists in the inequivalence of $\sigma$ and $\pi$-subsystems, in the comparison with the equivalence of Fe orbitals $d_{xz}$ and $d_{yz}$, considered in (42).

However, even in the given more simple case the task was solved the only by numerical methods. The main result is represented in Figure 8 in (42).

The magnetic excitation spectrum carries an information on the nature of a magnetism and the characteristics of the superconductivity. It has been discussed in the literature, that an observation of a sharp quasiparticle-like resonance peak in the spin fluctuation spectrum with the onset of superconductivity may strongly indicate a sign change in the gap structure caused by the superconducting coherence factors. It has been established, that in iron pnictides a strong spin resonance occurs in the $s^+$-wave SSt. The comparison of the ESR spectra, Figures 1 to 3, with theoretically calculated spectral function, presented in Figure 8 in (42) allows to suggest, that the spontaneous transition in the ESR response in the sample studied indicates on the transition to the SSt-state, which is coexisting with antiferromagnetic ordering, more strictly, with uncompensated antiferromagnetic ordering in the case considered. Therefore, it is the additional confirmation, that two lines - L-line and $R_b$-line - are assigned with uncompensated AFM-resonace observed in SSt-state. The inequivalence of the main characteristics of given lines can be attributed to strong inequivalence of two subsystems in NTs in a comparison with theoretically calculated in (42). It seems to be essential the result in the given work indicating on the appearance of the absorption with a very broad spectral distribution and with a peak-dip-hump feature, when the system becomes superconondducting. We have observed the derivative of the spectral function, which corresponds qualitatively by its integration to the spectral function with two peak-dip-hump features. It seems to be the consequence of different coupling of the resonance mode to fermions in $\pi$ and $\sigma$-subsystems, leading to splitting of the spectral function in two components. The spectral function, presented in Figure 8 in (42), was calculated numerically and the physical nature of the appearance of an absorption with a very broad spectral distribution has not been established. It has been done in the work (43). The authors have been studied theoretically the spin response in the normal and superconducting states of Fe-based pnictide superconductors. They showed that the resulting magnetic fluctuation spectrum calculated within random-phase approximation consists of two contributions. The first contribution is determined by the antiferromagnetic spin fluctuations peaked at wave vector $\vec{Q}_{AFM}$ arising in the result of the interband scattering. The second contribution comes from the intraband scattering and results in a broad continuum of the SDW fluctuations with a small momenta.

Further the authors of (42) indicate, that "detailed study of the magnetic and the electronic spectrum shows that the dispersion of the magnetic resonance mode in the nearly isotropic $s^+$ superconducting state exhibits an anisotropic propagating behavior in an upward pattern". Given conclusion is also in agreement with the experimental results in the samples studied, see (41) for details.

Further, the observation of superlinear dependence in the absorption kinetics, corresponding to L-line, Figure 4, is the strong evidence of the mobility of spin carriers (19) or the strong and the very fast spin energy transfer. Switching from the saturating behavior to the nonsaturating behavior with superlinear absorption kinetics of $R_b$-line, Figure 5, can be attributed to the decrease of the screening of the microwave magnetic field (and of the static magnetic field too) by $\pi$ subsystem when the microwave power is increased in the range $H_1/H_1^{(0)}\ 0.75-1$. Here we take in mind the reasonable suggestion that screening effect by $\pi$ subsystem is substantially more strong in the comparison with the screening effect by $\sigma$-subsystem and the microwave field penetrates more effectively at the low microwave power through $\sigma$-subsystem. In fact, the spin carriers in $\pi$ subsystem seem to be pinned at a low power, it is the consequence of the short penetration depth. The sharp increase of the absorption in the range $H_1/H_1^{(0)}\ 0.75-1$ is explained then by two factors - by depinning of spin carriers and by increasing of the number of spin carrirers, interacting with the microwave field in the given range, being to be the consequence of the increase of the penetration length.

In the favour of the SSt formation indicates the observation of a Dyson-like effect with an unusual angular dependence of an asymmetry extent A/B of L-line. It is qualitatively explained in (41). It seems to be also understandable the presence of some angular dependence of Q-factor. It is seen from Figure 10, that the relative change of Q-factor is small (although it is surely detectable), Q-factor

is nonmonotonically increased by the change of sample rotation angle from [011] to [100] the only in 1.115 times. Some decrease of Q-factor in the range (60 - 90) degrees from [100] can be explained by the existence of the nonsuperconducting part of NT-network, [which is confirmed by the detection of practically isotropic narrow line $R_n$] at the simultaneous decrease of the contribution in the total superconducting state of intraband transitions (see for details further), detected by very broad lines, which is decreasing in the given range (corresponding Figures are not represented). In other words, in the given range the redistribution of the resonance absorption contribution between superconducting and nonsuperconducting parts in the favour of the nonsuperconducting part, which characterises by some cavity Q-losses, although they are small, takes place. The fact, that the maximal Q-factor value is achieved in [100] direction can be explained in the following way. In the given direction the part of the microwave power can penetrate through the free unmodified diamond space between NTs to all sample volume, which is insulating and it is free from any magnetic impurities. That means, that the relative contribution of the nonsuperconducting part of the NT-network with some small Q-losses into total resonance and nonresonance parts of the interaction of all sample electronic subsystems with the microwave field has to be minimal, which is really observed.

The very pronounced angular dependence of the linewidth of L-line seems to be the most clear demonstration of Meissner effect. Meissner effect is expected to be very anisotropic in the sample studied, since, on the one hand, the superconductivity is suggested to be multicannel (see further), that is, it is determined by different mechanisms simultaneously. On the other hand, there are in the sample unmodified regions between NTs in NT-network, which strengthen the anisotropy of Meissner effect. So, near the [100] direction Meissner effect seems to be minimal, since static magnetic field $H_0$ can penetrate along NT axes both in inner NT space and in outer surrounding unmodified diamond regions. That ensures the minimal inhomogeneity of the magnetic field along all the nanotubes' surface and the minimal value of the linewidth, which really takes place. In other words, the effective thickness of superconducting layer seems to be less than the penetation depth value in Meissner effect. Then, the linewidth increase, which is starting from 5 degrees [the given value is the only approximate value, more precise measurements were not provided] can be explained by the increase of the effective thickness of the superconducting layer, since the individual static magnetic field line will intersect the big number of NTs even by the small deviation from the strict implantation direction. Let us remark once again, that our previous measurements show, that the inaccuracy in the implantaton directon by an implantation process does not exceed 1 degree, at the same time we have to remark, that the some inaccuracy can be in the experiment described in the determination of [100] direction in the sample rotation plane (which, however does not exceed 2 degrees). Then, the appearance of the branch in (5-40) degree range, where the growth of the linewidth of line L is observed, is explained by the inhomogeneity increase along individual static magnetic field line determined by Meissner effect. The given viewpoint correlates well with data on the angular dependence of the absorption intensity. It is seen from Figure 7, that the growth of the absorption intensity in (5-40) degree range is not pronounced, since, although the effective thickness of the operating region for the absorption process is increased, but the inhomogeneity of the amplitude of the magnetic component of the microwave field is also increased, being to be the consequence of Meissner effect too. In fact, the average value of the amplitude of magnetic component $H_1$ of the microwave field in the volume of the implanted region is decreased, resulting in the almost compensation of the effect of theb growth of the effective thickness of the absorbing layer. Starting from 40 degrees upto $\approx$ 70 degrees the processes of intraband transions become very effective [in AFM cannel the very broad lines are corresponding to given processes, it really takes place, the corresponding Figures are not represented, although the readers can compare the Figures 2 and 3 with the Figure 1]. It leads to the substantial decrease of the penetration depth, resulting in the substantial decrease of the effective thickness of absorbing layer. It means, that the part of NTs length along the individual static magnetic field line drop out from resonance conditions at all, being to be the consequence of screening both the static magnetic field and the microwave field. It is understandable, that both the absorption intensity and the linewidth of line L have to be decreasing, at that the appearance of absorption intensity

decreasing is evident (both the average value of $H_1$ and the effective number of absorbing spin carriers are decreasing). Linewidth decreasing is explained by the decrease of the range of static magnetic field, where the resonance conditions can be restored by the $H_0$ scan, being to be the consequence on more sharp $H_0$ -field strength damping to the same near zero-coordinate value along the penetration direction. It explains the decrease of inhomogeneity of $H_0$ -field, determined by Meissner effect and the corresponding linewidt decrease inthe given angle range in a natural way. Given conclusions correspond to experimental data, see Figures 7 and 8. The second branch of the linewidth growth, starting in the range 70-75 degrees from [100] direction, Figure 8, and the corresponding branch of the intensity growth, Figure 7, have the same origin, which has the linewidth and the absorption intensity growth, starting at $\approx$ 5 degrees. It is the direct consequence of the damping of intraband transions, taking place in the given range. It explains the resemblance of two branches of the linewidth growth, starting at $\approx$ 5 degrees and in the range 70-75 degrees from [100] direction, seen in Figure 8. The difference of analogous branches of the absorption intensity growth can be explained by different screening of the magnetic component $H_1$ of the microwave field in given ranges. Actually, when $H_0$ is near [100] direction, then the propagation direction for the microwave field is near [011] direction, that is, near the direction, which is transverse to nanotube axes. The given direction is characterised by the strong reflection and backscattering of the microwave power. At the same time, when $H_0$ is near [011] direction, then the propagation direction for the microwave field is near [100] direction, that is, near the direction, which is parallel to nanotube axes. In the given case the reflection and backscattering of the microwave power leads to its propagation along NT surface in the internanotube space.

Therefore, the observed angular dependences of the linewidth of line L and the absorption intensity, corresponding to the given line, become the clear qualitative explanation by taking into consideration the Meissner effect.

Let us give some simple evaluation of the penetration depth, based on the given experimental results. The effective diameter of NTs can be evaluated from the modification extent of the near surface implanted layer with the ion beam dose increase. It was surely established in previous studies, see, for instance, (20) that at $5 \times 10^{14}\ cm^{-2}$ ion integral fluence the entire modification takes place. Then in the approximation of an uniform nanotube distribution along the implantation sample surface and by neglecting of track canneling and nanotube overlapping, we obtain the diameter value, equal to $\approx$ 4.5 $\mathring{A}$. The effective distance between NT centers by the same suggestions at $5 \times 10^{13}\ cm^{-2}$ ion integral fluence is $\approx$ 14 $\mathring{A}$. Then, assuming that by the direction in 5 degrees the intersection length by an individual static magnetic field line achieves the penetration depth value, we obtain the number of the NTs intersected, equal to $\approx$ 250 [The length of the superconducting part of an individual NT was taken to be equal 2 $\mu m$. Although the strict value of the ratio of the lengths of superconducting and nonsuperconducting parts is unknown, given value seems to be suitable for the approximate evaluation.] Then, by using of an effective thickness for an individual NT, equal to interatomic distance in a graphene layer, that is 1.42 $\mathring{A}$ instead of intertube distance we obtain the value of the penetration depth in $\approx$ 18 nm. Naturally, the given evaluation gives the only order for the penetration depth value, however, the given evalution is coinciding in its order with the well known penetration depth, in particular, with Londons' length, which is equal to (in its order) $\sim$ 10 nm in superconducting metals.

Let us represent some additional arguments in favour of the interpretation above proposed. The very strong additional argument is the observation of the very pronounced Dyson-like effect itself, which, what is more, is observed by an unconventional A/B angular dependence. For a comparison, in a very similar NT-system, which was formed inside the channels of a non-magnetic insulating SAPO 5 zeolite crystal a Dyson effect was not observed (44). Let us give a detailed description of the given system preparation. According to (44) the sample preparation method involved a heat treatment of a SAPO 5 in an inert atmosphere (pyrolysis) and filling its pores with a suitable carbon source. It resulted in the presence of the NTs with the only three chiralities (5,0) (4,2) and (3,3), thus minimizing a chiral distribution. It has also been inferred that (5,0) and (3,3) chiral nanotubes were metallic (it

seems to be essential for the comparison with our results) and (4,2) nanotubes were semiconducting. Raman radial breathing mode (RBM) features indicated an average inner diameter of 0.4 nm for given single walled carbon nanotubes. From the optical polarized photoluminescence data, the arrays of SWNTs were found to align according to the channels of the zeolite crystal. The ESR samples studied in (44) imply that single walled carbon nanotubes are occluded inside the channels of a non-magnetic insulating SAPO 5 zeolite crystal. For reasons of a comparison, ESR observations have also been carried out on free standing SWCNTs obtained through a dissolution of the zeolite matrix in a aqueous acidic solution. At all the temperatures covered, a symmetric isotropic ESR signal was observed at zero-crossing g-value $g_c \approx 2.0025$, indicating on the absence of a Dyson effect.

The given comparison seems to be correct since a ion track surface is in fact SWCNT, at that the diameter of NTs is also comparable. Let us remark once again, that two kinds of SWCNTs in (44) were identified to be metallic. Therefore, even the given comparison seems to be sufficient to confirm the conclusion on the reality of AFM-SSt of NTs in our sample, since to observe any Dyson-like effect the conductivity has to be better than metallic.

To explain the symmetry character of the angular dependence of the strong absorption with very broad lines, let us consider the band model of NTs. For qualitative conclusions, it seems to be sufficient to consider the band model of graphene.

The first calculation of electronic states in a 2D lattice of carbon atoms with a honeycomb symmetry have been undertaken by Wallace (45) in 1947. Wallace used graphene to be a starting element for a description of bands in a bulk graphite. Taking into account the strong hybridization of $2s2p^2$ orbitals in the graphene plane, Wallace considered just the remaining $p$ orbital (oriented perpendicular to the crystal plane) to be responsible for the electronic band structure in the vicinity of the Fermi level and suggested a standard tight-binding approach. Considering the only the nearest-neighbour hopping parameter $\gamma_0$, a pair of $\pi$-bands is obtained (46)

$$E^*_\pi(\vec{k}) = -E_\pi(\vec{k}) = \gamma_0\sqrt{1 + 4\cos^2\frac{4k_y a_0}{2} + 4\cos\frac{4k_x\sqrt{3}a_0}{2}\cos\frac{4k_y a_0}{2}}, \tag{4.33}$$

which distinctly cross (touch) at two inequivalent $K$ and $K'$ points of the Brillouin zone. The strength of the nearest-neighbour hopping is 3.2 eV and the lattice constant $a_0$ = 0.246 nm is by a factor of $\sqrt{3}$ larger than the distance between the nearest carbon atoms.

So, in a pristine graphene, the Fermi level lies just at the touching (crossing) point (the Dirac or charge neutrality point) of $\pi^*$ and $\pi$ bands and graphene has a character of zero-band-gap semiconductor (semimetal). Band structure on some distance from Fermi level consist of six symmetric Dirac cones in the approach above considered, with vertices, which produce a regular hexagon, that is, with the angle distance from each other in $\pi/3$ relatively the hexagon center. The given structure is retained for NTs to the first order approximation, that seems to be substantial for the explanation of the observed experimental data in $\langle 100\rangle$-incorporated NTs, which are displaing an own symmetry, being to be different from a diamond lattice symmetry (see further).

Close to a given crossing (touching) point, the electronic bands are nearly linear and practically rotationally symmetric. In other words, the carrier dispersion relations take a simple form

$$E^*_\pi = -E_\pi \approx v_F\hbar|\vec{k}|, \tag{4.34}$$

where the momentum $\vec{k}$ is measured with respect to $K(K')$ point. The parameter $v_F$, having the dimension of a velocity, is directly related to the coupling strength (hopping integral) between the nearest carbon atoms: $v_F = \sqrt{3}a_0\gamma_0/(2\hbar)$. It is known, that the linearity of bands in graphene (in the vicinity of the $K$ and $K'$ points) implies, on the one hand, that the charge carriers' behavior in pristine graphene samples is like to the behavior of relativistic particles with a zero rest mass and the constant velocity $v_F$, equaled to $\approx 10^6 cms^{-1}$ in the given case. Given particles are often attributed

to massless Dirac fermions, and their behaviour is described by the effective Hamiltonian (46)

$$\hat{H} = v_F \begin{bmatrix} 0 & \hat{p}_x - i\hat{p}_y \\ \hat{p}_x + i\hat{p}_y & 0 \end{bmatrix} = v_F \hat{\vec{\sigma}} \hat{\vec{p}}, \tag{4.35}$$

which is equivalent to the Hamiltonian in the Weyl equation for real relativistic particles with a zero rest mass (originally for neutrinos) derived from the Dirac equation. On the other hand, the dispersion relation (4.34) is the key relation for a LL-behavior of an electronic system. Seemingly, the electronic system of graphene has to be considered, taking into account the results of the work (32), within the frames of the Luttinger liquid concept instead of the relativistic-like description of electronic states in graphene given by Hamiltonian (4.35). However, the Luttinger liquid concept was not used. It seems to be the striking example, that the Luttinger liquid concept is really inapplicable for the description of real electronic systems.

It is known, that the deviations from the relativistic model, briefly above described, become significant for states far away from the Dirac point, even if only the nearest neighbours in the tight-binding calculation are considered. Other deviations may arise when including the hopping integrals between next-nearest neighbours. For example, when taking into account the non-zero values of next-nearest hopping integrals, the nonlinearity is enhanced and Dirac cones become asymmetric with respect to the charge neutrality point. The most essential is that, that for the development of the description of the electronic states in pristine graphene was choosed the way, which is far from the LL (TLL) concept.

Qualitatively the characteristic features of angular dependencies of the parameters of ESR-spectra observed can be explained now in the following way. The quasiparticle spectral function, which describes the ESR spectrum observed is (42)

$$A(\vec{k}, \omega) = -\frac{1}{\pi} Im[\sum_a G^{aa}(\vec{k}, i\omega_n \to \omega + i\delta)] \tag{4.36}$$

with the dressed normal single-particle propagators $G^{aa}$ determined by solving the coupled Dyson-Gorkov equations, $\omega_n$ is bosonic Matsubara frequency, $\omega_n = 2n\pi T$. We see, that the spectral function depends on $\vec{k}$ in an explicit form. Further, the value of AFM vector $\vec{Q}$ is determined by $\vec{k}$-difference between inequivalent $K$ and $K'$ points of Dirac cones, that is by $\pi/3$, which is really experimentally displaying in angular dependencies of the absorption spectral distribution. In particular, it becomes to be understandable, why the absorption with very broad two lines is observed in the range of the angles near $\pi/3$ with the intensity maximum at $\pi/3$ and with the coincidence of peak-dip-hump features of both very broad lines at the given angle. Given conclusion followsfrom the quantIt is taken into account, that a periodical function in the wave vector $\vec{k}$-space has the same period in the coordinate $\vec{r}$-space.

We see from the foregoing theoretical consideration, that in the case considered the advantages of several mechanisms of the SSt formation can be joined. On the one hand, a s-wave mechanism, mediated by coupling of charge carriers with stretched phonon modes like to $MgB_2$, heavily boron doped diamond and sandwich S-Si-QW-S structures can be taking place. Moreover, just a crimped cylindrical shape allows to increase the strength of C-C bonds by the preservation of the high density of the states on FS, resulting from a low dimensionality (which seems to be intermediate between 1D and 2D). On the other hand, the multiband structure of valence and conductivity bands allows to realise the formation of AFM-SSt by means of the $s^+$-wave formation like to pnictides and additionally the $p$-wave formation. It seems to be a new mechanism - joint $s^+$-$p$-wave mechanism. Just the given mechanism is experimentally proved in the work presented. The independent on the dimerization coordinate an electron-electron repulsion (which can be both in static and dynamic) term seems to giving the contribution to the AFM-SSt formation by the given mechanism. The foregoing theoretical consideration allows to suggest also, that the usual s-wave BCS mechanism with the spin S = 0 Cooper pairing process of quasiparticles can produce an additional independent superconducting cannel. The detection of the given mechanism immediately by a magnetic resonance technique in

the superconductors of the first kind is labored, however it it is possible for the superconductors of the second kind, see, for instance (47). Along with the given mechanism, the s-wave BCS-like mechanism with the spin S = 1 Cooper pairing process of quasiparticles can, in principle, also take place. The attractive terms, which are proportional to the dimerization coordinate, can contribute to both BCS and BCS-like phonon-mediated mechanisms and to s-wave mechanisms, mediated by coupling of charge carriers with stretched phonon modes like to those ones established in $MgB_2$, heavily boron doped diamond and sandwich S-Si-QW-S structures. Further, the formation of $\sigma$-polaron lattice with AFM-ordering, which takes place, for instance, in the samples, implanted in $\langle 111 \rangle$ direction (20), leads also to a new possible mechanism of a AFM-SSt formation. It will be pure $s^+$-wave mechanism, like to those ones, taking place in many pnictides. The main feature, which differ the given mechanism from known ones is the other spatial distribution of delocalised spins. It is $\sigma$-polaron lattice instead of SDW.

Therefore, all the terms in the Taylor expansion of the electron-electron interaction above considered can contribute to the formation of SSt by different channels.

The switch to the SSt just in ESR conditions allows to explain the substantial broadening of ESR-lines, both, the rather large minimal value of the linewidth of L-line and $R_b$-line in the comparison with $R_n$-line in nonsuperconducting state, which seems to be partly coexisting in the sample studied (let us remember, that it is indicated by the presence of $R_n$-line in ESR-spectra simultaneously with the new lines L and $R_b$). Really, in the SSt with a momentum dependent SSt-gap an ESR linewidth $\Delta H$ is determined by a spin-lattice relaxation time $T_1$, $\Delta H \sim 1/T_1$, which is generally given by (see, for instance, (48))

$$\frac{(T_1T)^{-1}}{(T_1T)^{-1}_{T=T_c}} = \frac{2}{k_BT_c}\int\limits_0^\infty [N_s^2(E) + \alpha_c M_s^2(E)]f(E)[1-f(E)]dE, \tag{4.37}$$

where

$$N_s(E) = \frac{1}{4\pi}\int\limits_0^{2\pi}\int\limits_0^{\pi} \frac{E}{\sqrt{E^2 - |\Delta(\phi,\theta)|^2}}\sin\theta d\phi d\theta \tag{4.38}$$

$$M_s(E) = \frac{1}{4\pi}\int\limits_0^{2\pi}\int\limits_0^{\pi} \frac{\Delta(\phi,\theta)|}{\sqrt{E^2 - |\Delta(\phi,\theta)|^2}}\sin\theta d\phi d\theta, \tag{4.39}$$

where $N_s(E)$ and $M_s(E)$ are the density of states (DOS) for quasiparticles and the anomalous DOS originating from the coherence effect of the transition probability in the SSt, respectively, $\Delta(\phi,\theta)$ is SSt-gap. In a conventional $s$-wave SSt, the presence of $M_s(E)$ gives rise to $\Delta H$ just below $T_c$, since it usually has an isotropic gap with the same sign on the all Fermi surfaces. By contrast, in the unconventional $d$-wave and/or $p$-wave SSt-states, the $M_s(E)$ term is cancelled out by integrating over the momentum space on the SSt-gap. It seems to be explaining qualitatively the difference in linewidth values for $L$- and $R_b$ lines, which are proposed to be connected with $s$- and $p$-wave SSts cannels correspondingly, simultaneously realized in the sample studied. In the multiband system, the $N_s(E)$ and $M_s(E)$ terms in (4.37) are represented in the form ($N_s^h(E)$ + $N_s^e(E)$) and ($M_s^h(E)$ + $M_s^e(E)$), respectively, where the $N_s^h(E)$ and $N_s^e(E)$ are the DOS of the hole and electron FSs, respectively. In the case of the Fe-pnictides the $M_s(E)$-term is negligibly small. It was theoretically proposed that this result is accounted for on a basis of a nodeless $s^+$-wave pairing scenario assuming a sign reversal gap function, +$\Delta_h$ and -$\Delta_e$ on the hole and electron FSs, respectively. In cases, where the $\Delta_h$ and $\Delta_e$ have opposite signs, it is noteworthy that the $2M_s^h(E) \times M_s^e(E)$ component in $(M_s^h(E) + M_s^e(E))^2$ becomes negative. In particular, when assuming the well- nested FSs, it is anticipated that the sign-nonconserving interband scattering process ($+\Delta_h \leftrightarrow -\Delta_e$) may exceed the sign-conserving intraband scattering process ($+\Delta_h \leftrightarrow +\Delta_h$ and $\Delta_e \leftrightarrow \Delta_e$). The former process reduces the $M_s^2(E)$ term through the negative contribution of the $2M_s^h(E) \times M_s^e(E)$, whereas the latter process does not. Here, to deal with convoluted intraband and interband contributions in the

spin relaxation process the coefficient $\alpha_c$ in the expression (4.37) is introduced phenomenologically. It takes a value $\alpha_c \leq 1$ depending on the weight of the interband contribution. Really, the substantial more large value of the linewidth $L$ in AFM-SSt in the comparison with $R_b$-line means, that the coefficient $\alpha_c$ in (4.37) is nonzero. Moreover, the increase of the linewidth of the $R_b$-line in the comparison with the $R_n$-line means, that there is the additional mechanism of line broadening in the addition to above considered. It is determined by Meissner effect and it always will be take place by the transition to SSt independently on the superconductivity mechanism.

More detailed studies are necessary to clarify all the processes leading to the room temperature superconductivity and to establish the partial contributions of all the mechanisms considered. In particular, all known models cannot explain the observation of the transition to AFM-SSt just in magnetic spin resonance conditions. To explain the role of spin resonance conditions for the switch to the AFM-SSt we have to take into account the quantum nature of EM-field in the radiospectroscopy range. The given task has been solved in (49), where matrix-operator difference-differential equations for a dynamics of spectroscopic transitions in 1D multiqubit exchange coupled (para)magnetic and optical systems by strong dipole-photon and dipole-phonon coupling are derived within the framework of the quantum field theory. It has been established, that in the model considered the relaxation processes are of a pure quantum character, which is determined by the formation of the coherent system of the resonance phonons and by the appearence along with the absorption process of EM-field energy of the coherent emission process, acompanying by a new physical phenomenon - phonon Rabi quantum oscillations, which can be time-shared. For the case of the radiospectroscopy it corresponds to the possibility of the simultaneous observation along with (para)magntic spin resonance the acoustic spin resonance.

Let us represent the brief review for given results with the same aim, that is, for the convenience of readers. In the work (50) the system of difference-differencial equations for a dynamics of spectroscopic transitions for both a radio- and an optical spectroscopy for the model, representing itself the 1D-chain of N two-level equivalent elements coupled by an exchange interaction (or its optical analogue for the optical transitions) between themselves and interacting with a quantized EM-field and a quantized phonon field has recently been derived. The model presented in (50) differs from Tavis-Cummings model (51) the most essentialy by the inclusion into consideration of a quantized phonon system, describing the relaxation processes from a quantum field theory position. Seven equations for the seven operator variables, describing a joint system $\{$field + matter$\}$ were presented in a matrix form by three matrix equations.

However, it is shown in (49), that by strong electron-photon coupling and strong electron-phonon coupling quite another picture of quantum relaxation processes becomes to be possible in the comparison with the picture, obtained in (50). It is argued in the given work the following. The definition of the wave function of the chain system, interacting with a quantized EM-field and with a quantized lattice vibration field, to be vector of the state in Hilbert space over quaternion ring, that is a quaternion function of a quaternion argument, leads to the Lorentz invariance of the equations obtained in (50) and to the possibility of the transfer to observables. In fact, in the work cited, the main role of the spin vector for the quantum state description was taken into account. Since the spin vector is the vector of the state [in Hilbert space over a quaternion ring] with an accuracy to a normalization factor of any 1D quantum system, interacting with a quantized electromagnetic field, all the components of the vector of the state, that is, the components of the spin vector, being to be peer components, have to be taken into consideration. At the same time, the Hamiltonian, given in (50) describes in fact the only part of an interaction with a phonon field, which corresponds the only to $z$-component of the vector of the state. The interaction of a dipole subsystem with a phonon field, corresponding to x- and y-components of the vector of the state of a dipole subsystem (that is, to $S^+$- and $S^-$ components of the spin of a matter subsystem, since they are proportional to two linear combinations of peer $x$- and $y$-components of the vector of the state of the system considered) was taken into consideration in (49). Therefore, the following Hamiltonian was obtained in a natural way

$$\hat{\mathcal{H}} = \hat{\mathcal{H}}^C + \hat{\mathcal{H}}^F + \hat{\mathcal{H}}^{CF} + \hat{\mathcal{H}}^{Ph} + \hat{\mathcal{H}}^{CPh}, \tag{4.40}$$

where $\hat{\mathcal{H}}^C$ is the chain Hamiltonian by the absence of the interaction with an EM-field, $\hat{\mathcal{H}}^F$ and $\hat{\mathcal{H}}^{Ph}$ are the photon and phonon field Hamiltonians correspondingly, $\hat{\mathcal{H}}^{CF}$ and $\hat{\mathcal{H}}^{CPh}$ are, accordingly, Hamiltonians, describing the interaction between a quantized EM-field and an electronic subsystem of an atomic chain and between a quantized phonon field and an electronic subsystem of an atomic chain. Then, the equations of the motion for the spectroscopic transition operators $\hat{\vec{\sigma}}_l$, for quantized EM-field operators $\hat{a}_{\vec{k}}$, $\hat{a}^+_{\vec{k}}$ and for phonon field operators $\hat{b}_{\vec{q}}$, $\hat{b}^+_{\vec{q}}$ are the following.

$$\frac{\partial}{\partial t}\begin{bmatrix}\hat{\sigma}_l^-\\ \hat{\sigma}_l^+\\ \hat{\sigma}_l^z\end{bmatrix} = 2\,\|g\|\begin{bmatrix}\hat{F}_l^-\\ \hat{F}_l^+\\ \hat{F}_l^z\end{bmatrix} + ||\hat{R}^{(\lambda^z)}_{\vec{q}l}|| + ||\hat{R}^{(\lambda^\pm)}_{\vec{q}l}|| \tag{4.41}$$

$$\frac{\partial}{\partial t}\begin{bmatrix}\hat{a}_{\vec{k}}\\ \hat{a}^+_{\vec{k}}\end{bmatrix} = -i\omega_{\vec{k}}||\sigma^z_P||\begin{bmatrix}\hat{a}_{\vec{k}}\\ \hat{a}^+_{\vec{k}}\end{bmatrix} + \frac{i}{\hbar}\begin{bmatrix}-\sum\limits_{l=1}^{N}(\hat{\sigma}_l^+ + \hat{\sigma}_l^-)v^*_{l\vec{k}}\\ \sum\limits_{l=1}^{N}(\hat{\sigma}_l^+ + \hat{\sigma}_l^-)v_{l\vec{k}}\end{bmatrix}, \tag{4.42}$$

$$\frac{\partial}{\partial t}\begin{bmatrix}\hat{b}_{\vec{k}}\\ \hat{b}^+_{\vec{q}}\end{bmatrix} = -i\omega_{\vec{q}}||\sigma^z_P||\begin{bmatrix}\hat{b}_{\vec{q}}\\ \hat{b}^+_{\vec{q}}\end{bmatrix} + \frac{i}{\hbar}\begin{bmatrix}-\sum\limits_{l=1}^{N}\{\lambda^z_{\vec{q}l}\hat{\sigma}_l^z + \lambda^\pm_{\vec{q}l}(\hat{\sigma}_l^+ + \hat{\sigma}_l^-)\}\\ \sum\limits_{l=1}^{N}\{\lambda^z_{\vec{q}l}\hat{\sigma}_l^z + \lambda^\pm_{\vec{q}l}(\hat{\sigma}_l^+ + \hat{\sigma}_l^-)\}\end{bmatrix}, \tag{4.43}$$

where matrix $||\hat{R}^{(\lambda^z)}_{\vec{q}l}||$ is

$$||\hat{R}^{(\lambda^z)}_{\vec{q}l}|| = \frac{1}{i\hbar}\begin{bmatrix}2\hat{B}^{(\lambda^z)}_{\vec{q}l}\hat{\sigma}_l^-\\ -2\hat{B}^{(\lambda^z)}_{\vec{q}l}\hat{\sigma}_l^+\\ 0\end{bmatrix} \tag{4.44}$$

with $\hat{B}^{(\lambda^z)}_{\vec{q}l}$, which is given by

$$\hat{B}^{(\lambda^z)}_{\vec{q}l} = \sum_{\vec{q}}[(\lambda^z_{\vec{q}l})^*\hat{b}^+_{\vec{q}} + \lambda^z_{\vec{q}l}\hat{b}_{\vec{q}}]. \tag{4.45}$$

Matrix $||\hat{R}^{(\lambda^\pm)}_{\vec{q}l}||$ is

$$||\hat{R}^{(\lambda^z)}_{\vec{q}l}|| = \frac{1}{i\hbar}\begin{bmatrix}-\hat{B}^{(\lambda^\pm)}_{\vec{q}l}\hat{\sigma}_l^z\\ \hat{B}^{(\lambda^\pm)}_{\vec{q}l}\hat{\sigma}_l^z\\ \hat{B}^{(\lambda^\pm)}_{\vec{q}l}(\hat{\sigma}_l^+ - \hat{\sigma}_l^-)\end{bmatrix}, \tag{4.46}$$

where $\hat{B}^{(\lambda^\pm)}_{\vec{q}l}$ is

$$\hat{B}^{(\lambda^\pm)}_{\vec{q}l} = \sum_{\vec{q}}[(\lambda^\pm_{\vec{q}l})^*\hat{b}^+_{\vec{q}} + \lambda^\pm_{\vec{q}l}\hat{b}_{\vec{q}}]. \tag{4.47}$$

The parameters $\lambda_{\vec{q}}^{z}$ and $\lambda_{\vec{q}}^{\pm}$ are electron-phonon coupling constants, which characterise respectively the interaction of a electron subsystem of jth chain unit, corresponding to $z$- component of its vector of the state (or $S_j^z$) and the interaction of a electron subsystem of jth chain unit, corresponding to the $\pm$- componenst of its vector of the state (or $S_j^+$- and $S_j^-$ components of the spin of jth chain unit). It seems to be understandable, that they can be different in the general case. Moreover, in order to take into account the interaction with both equilibrium and nonequilibrium phonons both the electron-phonon coupling constants have to be complex numbers.

The operator $\hat{\vec{\sigma}}_l$

$$\left[\begin{array}{c} \hat{\sigma}_l^- \\ \hat{\sigma}_l^+ \\ \hat{\sigma}_l^z \end{array}\right] = \hat{\vec{\sigma}}_l = \hat{\sigma}_l^- \vec{e}_+ + \hat{\sigma}_l^+ \vec{e}_- + \hat{\sigma}_l^z \vec{e}_z \tag{4.48}$$

is the vector-operator of spectroscopic transitions for $l$th chain unit, $l = \overline{2, N-1}$ (50), which was represented in the matrix form. Its components, that is, the operators

$$\hat{\sigma}_v^{jm} \equiv |j_v\rangle\langle m_v| \tag{4.49}$$

are set up in a correspondence to the states $|j_v\rangle$,$\langle m_v|$, where $v = \overline{1, N}$, $j = \alpha, \beta$, $m = \alpha, \beta$. For instance, the relationships for commutation rules are

$$[\hat{\sigma}_v^{lm}, \hat{\sigma}_v^{pq}] = \hat{\sigma}_v^{lq}\delta_{mp} - \hat{\sigma}_v^{pm}\delta_{ql}. \tag{4.50}$$

Further

$$\left[\begin{array}{c} \hat{F}_l^- \\ \hat{F}_l^+ \\ \hat{F}_l^z \end{array}\right] = \hat{\vec{F}} = \left[\hat{\vec{\sigma}}_l \otimes \hat{\vec{\mathcal{G}}}_{l-1,l+1}\right], \tag{4.51}$$

where vector operators $\hat{\vec{\mathcal{G}}}_{l-1,l+1}$, $l = \overline{2, N-1}$, are given by the expressions

$$\hat{\vec{\mathcal{G}}}_{l-1,l+1} = \hat{\mathcal{G}}_{l-1,l+1}^- \vec{e}_+ + \hat{\mathcal{G}}_{l-1,l+1}^+ \vec{e}_- + \hat{\mathcal{G}}_{l-1,l+1}^z \vec{e}_z, \tag{4.52}$$

in which

$$\hat{\mathcal{G}}_{l-1,l+1}^- = -\frac{1}{\hbar}\sum_{\vec{k}} \hat{f}_{l\vec{k}} - \frac{J}{\hbar}(\hat{\sigma}_{l+1}^- + \hat{\sigma}_{l-1}^-), \tag{4.53a}$$

$$\hat{\mathcal{G}}_{l-1,l+1}^+ = -\frac{1}{\hbar}\sum_{\vec{k}} \hat{f}_{l\vec{k}} - \frac{J}{\hbar}(\hat{\sigma}_{l+1}^+ + \hat{\sigma}_{l-1}^+), \tag{4.53b}$$

$$\hat{\mathcal{G}}_{l-1,l+1}^z = -\omega_l - \frac{J}{\hbar}(\hat{\sigma}_{l+1}^z + \hat{\sigma}_{l-1}^z). \tag{4.53c}$$

Here operator $\hat{f}_{l\vec{k}}$ is

$$\hat{f}_{l\vec{k}} = v_{l\vec{k}}\hat{a}_{\vec{k}} + \hat{a}_{\vec{k}}^+ v^*{}_{l\vec{k}}. \tag{4.54}$$

In relations (4.53) $J$ is the exchange interaction constant in the case of magnetic resonance transitions or its optical analogue in the case of optical transitions, the function $v_{l\vec{k}}$ in (4.54) is

$$v_{l\vec{k}} = -\frac{1}{\hbar} p_l^{jm}(\vec{e}_{\vec{k}} \cdot \vec{e}_{\vec{P}_l}) \mathfrak{E}_{\vec{k}} e^{-i\omega_{\vec{k}}t + i\vec{k}\vec{r}}, \tag{4.55}$$

where $p_l^{jm}$ is the matrix element of the operator of the magnetic (electric) dipole moment $\vec{P}_l$ of *l-th* chain unit between the states $|j_l\rangle$ and $|m_l\rangle$ with $j \in \{\alpha, \beta\}$, $m \in \{\alpha, \beta\}$, $j \neq m$, $\vec{e}_{\vec{k}}$ is the unit polarization vector, $\vec{e}_{\vec{P}_l}$ is unit vector along $\vec{P}_l$-direction, $\mathfrak{E}_{\vec{k}}$ is the quantity, which has the dimension of a magnetic (electric) field strength, $\vec{k}$ is the quantized EM-field wave vector, the components of which get a discrete set of values, $\omega_{\vec{k}}$ is the frequency, corresponding to the $\vec{k}$th mode of EM-field, $\hat{a}_{\vec{k}}^+$ and $\hat{a}_{\vec{k}}$ are EM-field creation and annihilation operators correspondingly. In the suggestion, that the contribution of a spontaneous emission is relatively small (which is always takes place in a radiospectroscopy), $p_l^{jm} = p_l^{mj} \equiv p_l$, where $j \in \{\alpha, \beta\}$, $m \in \{\alpha, \beta\}$, $j \neq m$. Further, $\hat{b}_{\vec{q}}^+$, $\hat{b}_{\vec{q}}$ are the creation and annihilation operators of the phonon with the impulse $\vec{q}$ and with the energy $\hbar\omega_{\vec{q}}$ correspondingly. In the equations (4.42) and (4.43) $\|\sigma_P^z\|$ is Pauli $z$-matrix, $\|g\|$ in the equation (4.41) is a diagonal matrix, numerical values of its elements are dependent on the basis choice. It is at an appropriate basis

$$\|g\| = \begin{bmatrix} 1 & 0 & 0 \\ 0 & 1 & 0 \\ 0 & 0 & 1 \end{bmatrix}. \tag{4.56}$$

The right hand side expression in (4.51) is the vector product of vector operators. It can be calculated in accordance with the expression

$$\left[\hat{\vec{\sigma}}_l \otimes \hat{\vec{\mathcal{G}}}_{l-1,l+1}\right] = \frac{1}{2}\begin{vmatrix} \vec{e}_- \times \vec{e}_z & \hat{\sigma}_l^- & \hat{\mathcal{G}}_{l-1,l+1}^- \\ \vec{e}_z \times \vec{e}_+ & \hat{\sigma}_l^+ & \hat{\mathcal{G}}_{l-1,l+1}^+ \\ \vec{e}_+ \times \vec{e}_- & \hat{\sigma}_l^z & \hat{\mathcal{G}}_{l-1,l+1}^z \end{vmatrix}', \tag{4.57}$$

that is, by using of the known expression for an usual vector product with the additional coefficient $\frac{1}{2}$ the only, which is appeared, since the products of two components of two vector operators are replaced by anticommutators of corresponding components. The given detail is mapped by the symbol $\otimes$ in (4.51) and by the symbol $'$ in the determinant (4.57).

The terms like to the right hand side terms in (4.43) were used in so called "spin-boson" Hamiltonian (53) and in so called "independent boson model" (54). Given models were used to study phonon effects in a single quantum dot within a microcavity (55), (56), (57), (58), (59). So, it has been shown in (58), (59), that the presence of the term in the Hamiltonian (50)

$$\hat{\mathcal{H}}^{CPh} = \sum_{j=1}^{N}\sum_{\vec{q}} \lambda_{\vec{q}}(\hat{b}_{\vec{q}}^+ + \hat{b}_{\vec{q}})\hat{\sigma}_j^z, \tag{4.58}$$

which coincides with the corresponding term in the Hamiltonian in (58), (59) at $N = 1$ [the contribution of the given term to the equations for spectroscopic transitions is $\pm\sum_{l=1}^{N} \hat{\sigma}_l^z \lambda_{\vec{q}}$, see the equation (4.43), (note, that the equations for spectroscopic transitions were not derived in above cited works (55), (56), (57), (58), (59))] leads the only to the exponential decrease of the magnitude of quantum Rabi oscillations with the increase of the electron-phonon coupling strength and even to their supression at relatively strong electron-phonon coupling.

Thus, the QFT model for the dynamics of spectroscopic transitions in a 1D multiqubit exchange coupled system was generalized by taking into account, that a spin vector is proportional to a quaternion vector of the state of any relativistic quantum system [the joint matter + EM-field system has to be referred to relativistic systems] in a Hilbert space defined over a quaternion ring and, consequently, all the spin components has to be taken into account. The new quantum phenomenon was predicted in (49). The prediction results from the structure of the equations derived and it consists in the following. The coherent system of the resonance phonons, that is, the phonons with the energy, equaled to the resonance photon energy can be formed by a resonance, that can lead to an appearance along with Rabi oscillations determined by spin (electron)-photon coupling with the frequency $\Omega^{RF}$ of Rabi oscillations determined by spin (electron)-phonon coupling with the frequency $\Omega^{RPh}$. In other

words, QFT model predicts the oscillation character of the quantum relaxation, that is, the quite different character in comparison with phenomenological and semiclassical Bloch models. Moreover, if $\mid \lambda_{\vec{q}l}^{\pm} \mid < g$ the second Rabi oscillation process will be observed by the stationary state of two subsystems $\{$EM-fied + magnetic (electric) dipoles$\}$, that is, it will be registered in a quadrature with the first Rabi oscillation process. It can be experimentally detected even by means of stationary spectroscopy methods.

The second quantum Rabi oscillation process is governed by the formation of the coherent system of the resonance phonons. Therefore, along with the absorption process of a EM-field energy the coherent emission process can take place. Both the quantum Rabi oscillation processes can be time-shared. For the case of a radiospectroscopy it corresponds to the possibility of the simultaneous observation along with (para)magnetic spin resonance the acoustic spin resonance.

The predicted phenomenon of the formation of the coherent system of the resonance phonons can find the number of practical applications, in particular, it can be used by an elaboration of various logic quantum systems including quantum computers and quantum communication systems.

The appearance of a coherent system of the resonance hypersound phonons with the relatively high energy seems to be crucial for the switch of the electronic system of NTs in the samples studied to AFM-SSt. Really, let us consider the most simple example - the BCS s-wave mechanism of a superconductivity. It is taking place, when the interaction between electrons, realised through the phonon subsystem, will be attractive. In its turn, the given interaction is attractive, when the energy difference between the electron states involved is less than phonon energy $\hbar\omega_{ph}$ (25). In other words, the most significant contribution to the attractive interaction energy is given by short-wavelength phonons.

Therefore, the appearance of a coherent system of rather high energetic hypersound phonons in electtron spin resonance conditions seems to be having the key role for the switch of the NTs-network in the sample studied to the state, characterised by the superconductivity and the uncompensated antiferromagnetism. On the other hand, it is the strong argument, that phonon-mediated mechanisms give the substantial contribution to the total superconducting state.

Let us remark, that there are additional results in favour of the model proposed, represented in (41). The phenomenon of the ferrimagnetic spin wave resonance [uncompensated antiferromagnetic spin wave resonance] has been established [for the first time in the magnetic resonance spectroscopy] by a more detailed analysis of the spectra observed. The fact itself of an observation of an uncompensated antiferromagnetic spin wave resonance (SWR) is the direct proof of the formation of antiferromagnetic ordering [uncompensated]. The spin wave resonance observed has two main peculiarities.

1.The opposite deviation of the asymmetry extent ratio A/B from 1 of resonance modes in comparison with the main AFM mode, at that, the given deviation increases with the mode number increase.

It is the result, which allowed to exclude from the consideration the usual Dyson effect. The given peculiarity of the ferrimagnetic spin wave resonance was explained qualitatively by the existence of nodes like to the explanation of the asymmetry extent of the resonance lines in $d_{x^2-y^2}$ superconductors.

2.The substantial increase of the intensity of ferrimagnetic spin wave resonance modes with mode number increase.

Let us remark, that the intensity conservation law for spin wave resonance modes was found for NTs incorporated in diamond matrix with other implantation directions (18), for carbynoids and for some organic quasi-1D substances (polyvinylidenehalogenides - PVDF) (21). In the other earlier known cases, for instance, by a spin wave resonance in ferromagnetic metals, the intensity of spin wave resonance modes is decreasing with mode number increasing, see, for example, Figure 1 in (60). The peculiarity observed in the sample studied is explained by taking into account the presence of the magnetic fluctuation spectrum consisting of the continuum of the AFM spin fluctuations peaked at AFM vector $\vec{Q}$. In the case of a spin wave resonance wave, the value $|\vec{q}| \neq 0$ and $|\vec{q}|$ is increasing with the mode number increase, being to be coming near to the value of $|\vec{Q}|$. Then the dynamical magnetization will be determined by the Fourier component of the magnetic fluctuation field with the frequency, coinciding with the operating microwave frequency of the spectrometer. The given

component is added to the dynamical magnetization produced by the magnetic component of a microwave field used and it determines the mode intensity growth with an unusual asymmetry extent.

The observation of the only peculiarities of spin wave resonance above indicated seemed to be sufficient to insist on the formation in NTs' network of the sample studied of $s^+$-superconductivity at room temperature, coexisting with uncompensated antiferromagnetic ordering.

The results above discussed can be considered to be the basis for the method of identification of superconducting states, coexisting with a magnetism the only on the base ESR spectroscopy. Let us remark that the similar conclusion concerning the appplication of an ESR spectroscopy for the identification of a superconductivity [especially of superconductors, where a Josephson-vortex system can be formed] and for substantially more deep its study in comparison with electrical methods has been proposed earlier in (47) and references therein, see also review article by Shaltiel (62). Cited works show that an electron paramagnetic resonance spectrometer is a powerful tool to investigate properties of superconductors. Since superconducting systems are not conventional paramagnetic substances, the EPR signals can be not originate from the usual resonant absorption, namely magnetic dipolar transitions between spin levels. It is accentuated in (47) that it seems to be essential in analyzing the experimental results, to explore the mechanism that induces the EPR signals. Indeed, by detailed experimental and theoretical studies of the EPR spectra of different high $T_c$ superconductors, it was possible to solve the given task and new unknown properties of superconductors were obtained.

An accepted assumption in analyzing of experimental results obtained by an EPR-technique is that the role of the AC field is only to introduce weak oscillating variations in the magnitude of the DC magnetic field, that is, the AC field is usually referred to be the modulating magnetic field. However, it is shown in (47), (62), that the AC field does not just result in a modulation of the microwave signal dependent of the modulated static field like in a usual EPR experiment, but in superconductors it may also induce an additional mechanism of a microwave power dissipation. The reference AC phase of the lock-in-detector (LID) is adjusted for usual EPR measurements to yield the optimum paramagnetic resonance signal. However in case of the microwave dissipation observed in anisotropic superconductors this adjustment turns out to be not appropriate. Variations in the signal phase were observed when varying the magnitude of the variables - DC magnetic field, temperature, sample orientation and others. This effect necessitates a procedure where the LID phase has to be adjusted, throughout the measuring process, to be in-phase with the AC phase. To overcome this problem, conducted during the measuring process, the measurements have to be performed in steps of the variables involved, and at each step the LID phase had to be adjusted accordingly.

Let us remark, that similar conclusions, concerning the additional role of AC field, have been done in (16), (19), (18), (61), where by means of the study of the EPR-signal dependence on the frequency of AC field the nature of absorbing centers in some quasi-one-dimensional structures and the mechanisms of the energy transfer from spin system to surrounding lattice were established.

Futher, it is concluded in (47), (62), that EPR spectrometers can be used to search for superconducting materials, to determine their $T_c$, to study a resistivity in superconductors, and to investigate the effects of various parameters on the sample resistivity, without applying wiring contacts. It is in full agreement with our conclusion aforesaid, which was obtained independently (we get to know on the results, published in (47), (62) quite recently). In (47), (62) the mechanism of the EPR signal appearence by the presence of AC-field was established. It is the following - the AC modulation field induces eddy currents that apply a Lorentz force that induces the motion of fluxons in the high anisotropy superconductors Bi2212 and Bi2223. Their motion interacts with the microwaves and induces the observed signal. The analysis of the results allowed to establish the properties of Josephson vortices in high anisotropy superconductors. Two prominent achievements are indicated in(47):

(a) by means of field cooling and zero-field cooling experiments a memory effect was discovered and a corresponding phase diagram of the Josephson-vortex system was derived.

(b) from angular dependent measurements pinning of the Josephson vortices by Abricosov vortices was established.

Therefore, the results described in (47), (62) and the results presented in the given paper are

supplementing each other regarding the application of an ESR spectroscopy for superconductor studies.

# 5 Conclusions

The formation in carbon NTs, produced by high energy ion beam modification of diamond single crystals in $\langle 100 \rangle$ direction and representing themselves the surface of ion tracks, of uncompensated antiferromagnetic ordering coexisting with superconductivity at room temperature is argued. It is based on ESR studies. A number of peculiarities has been observed for the first time in a radiospectroscopy. The main results are the following.

1.It is the fact itself of the switch in resonance conditions to another rather stable state. It was shown, that the new state is defined by uncompensated antiferromagnetic ordering coexisting with the superconductivity. It is characterised spectroscopically by the appearence of two new rather broad anisotropic lines, designated L and $R_b$, which have, however, quite different spectroscopic properties, and by two very broad intensive lines.

2.The dependence of the absorption amplitude of the right broad line $R_b$ in the ESR spectrum of NTs on the magnetic component of a microwave field is strongly nonlinear. It is characterised for the values of the relative magnetic component of a microwave field $H_1/H_1^{(0)}$ in the range (0-0.75) by a usual saturating law, but in the range (0.75-1) it acquires a prominent superlinear nonsaturating character.

3.The unusual angular dependence of an asymmetry extent, which cannot be described within the framework of the Dyson theory.

4.Main details in very pronounced angular dependencies of the linewidth of the left line L and the intesity of the absorption, corresponding to the given line are exlained by the corresponding angular dependence of Meissner effect. It has been showed, that the broadening mechanism, determined by Meissner effect, will take place for any paramagnetic, or magnetically ordered system, localised in superconducting region, that is, the given broadening mechanism is universal. It is established for the first time in radiospectroscopy.

5.The penetration depth of the static magnetic field was evaluated to be equal $\approx$ 18 nm.

6.The difference in linewidths of the lines L and $R_b$ is analysed within the frames of the relaxation theory in superconducting state (SSt), which takes into account the anomalous density of states (DOS) originating from the coherence effect of the transition probability in the SSt. DOS, originating from the coherence effect gives rise to the linewidth of the line L, which is responsible for the $s^+$ branch of the mixed $s^+p$-wave superconductivity. At the same time, in the p-wave SSt the coherence effect is cancelled out by integrating over the momentum space on the SSt-gap, that is, it does not give rise to the linewidth of the line $R_b$, which is responsible for $p$ branch.

7. The Hamiltonian for the mathematical description of the phenomenon observed is built. It is based on the concept of 1D Fermi liquid for electronic states of quasi-1D systems, the concept was developed earlier, however, it is shortly reviewed in the given paper.

8.The analysis of the concept of 1D Fermi liquid allowed to propose a number of the other possible mechanisms of the SSt formation in the sample studied. On the one hand, s-wave mechanism, mediated by coupling of charge carriers with stretched phonon modes like to the superconductivity mechanism in $MgB_2$, heavily boron doped diamond and sandwich S-Si-QW-S structures can be taking place. Moreover, just the crimped cylindrical shape of NTs allows to increase the strength of C-C bonds by the preservation of the high density of the states on FS, resulting from the low dimensionality of the NT-structure. On the other hand, the multiband structure of valence and conductivity bands allows to realise the formation of AFM-SSt by means of the $s^+$-wave formation like to pnictides and additionally the $p$-wave formation. It seems to be new mechanism - the joint $s^+$-$p$-wave mechanism. Just the given mechanism is experimentally proved. The independent on the dimerization coordinate electron-electron repulsion terms in the Hamiltonian proposed are proposed to be giving the contribution

to the AFM-SSt formation by the given mechanism. The foregoing theoretical consideration allows to suggest also, that the usual s-wave BCS mechanism with the spin S = 0 Cooper pairing process of quasiparticles can produce the additional independent superconducting cannel. Along with the given mechanism, the s-wave BCS-like mechanism with the spin S = 1 Cooper pairing process of quasiparticles can in principle also take place. The attractive terms in the Hamiltonian, which are proportional to the dimerization coordinate, can contribute to the BCS and BCS-like phonon-mediated mechanisms and to s-wave mechanisms, mediated by coupling of charge carriers with stretched phonon modes like to those ones established in $MgB_2$, heavily boron doped diamond and sandwich S-Si-QW-S structures. Further, the formation of $\sigma$-polaron lattice with AFM-ordering, which can take place in the NTs, leads to the new possible mechanism of the AFM-SSt formation. It will be pure $s^+$-wave mechanism, like to those ones taking place in many pnictides. The main feature, which differ the given mechanism from known ones is the other spatial distribution of delocalized spins. It is a $\sigma$-polaron lattice instead of a spin density wave.

9.Especially interesting seems to be the role of an external quantized EM-field, which proposed to be responsible for the switch to SSt by means of the formation of coherent long-lived systems of resonance hypersound phonons. The corresponding quantum field theory was proposed something earlier, however, the brief review is given. Based on the given result, we can conclude, that the quantized radiospectrospy-range EM-field seems to be the working constituent for the realization of a room temperature SSt. On the other hand, it is considered to be the strong argument of the participation in the SSt-formation of BCS or BCS-like mechanisms (maybe the only at the stage of a transitional process). Thus, the room temperature SSt in $\langle 100 \rangle$-NTs, incorporated in a diamond matrix can be formed in the result of the participation of several mechanisms.

# Competing Interests

The authors declare that no competing interests exist.

# References

[1] Jun Nagamatsu, Norimasa Nakagawa, Takahiro Muranaka, Yuji Zenitani, Jun Akimitsu. Superconductivity at 39 K in Magnesium Diboride, Nature. 2001;410:63-64. DOI:10.1038/35065039

[2] An JM, Pickett WE. Superconductivity of MgB2: Covalent Bonds Driven Metallic, Phys. Rev. Lett. 2001;86:4366-4369.

[3] Kortus J, Mazin II, Belashchenko KD, Antropov VP, Boyer LL. Superconductivity of Metallic Boron in MgB2. Phys. Rev. Lett. 2001;86:4656-4659.

[4] Kong Y, Dolgov OV, Jepsen O, Andersen OK. Electron-Phonon Interaction in the Normal and Superconducting States of $MgB_2$. Phys. Rev. B. 2001;64:020501-4(R).

[5] Ekimov EA, Sidorov VA, Bauer ED, Mel'nik NN, Curro NJ, Thompson JD, Stishov SM, Superconductivity in Diamond, Nature. 2004;428:542-545. DOI:10.1038/nature02449

[6] Takano Y, Nagao M, Kobayashi K, Umezawa H, Sakaguchi I, Tachiki M, Hatano T, Kawarada H. Appl. Phys. Lett. 2004;85:2581.

[7] Blase X, Adessi Ch, Connetable D, Role of the Dopant in the Superconductivity of Diamond. Phys. Rev. Lett. 2004;93:237004-4.

[8] Lee KW, Pickett WE. Superconductivity in Boron-Doped Diamond. Phys. Rev. Lett. 2004;93:237003-4.

[9] Kawaji H, Horie HO, Yamanaka S, Ishikawa M. Superconductivity in the Silicon Clathrate Compound $(Na, Ba)_x Si_{46}$. Phys. Rev. Lett. 1995;74:1427-1429.

[10] Bagraev NT, Gehlhoff W, Klyachkin LE, Malyarenko AM, Romanov VV. Superconductivity in Silicon Nanostructures. arXiv:0806.2800v1 [cond-mat.supr-con]

[11] Kamihara Y, Watanabe T, Hirano M, Hosono H. Iron-Based Layered Superconductor $La[O_{1-x}F_x]FeAs$ (x = 0.05-0.12) with $T_c$ = 26 K. J. Am. Chem. Soc. 2008;130(N11):3296-3297. DOI: 10.1021/ja800073m

[12] Chubukov AV, Efremov DV, Eremin I, Magnetism, Superconductivity and Pairing Symmetry in Iron-Based Superconductors. Phys. Rev. B. 2008;78:134512-134512-10.

[13] Erchak DP, Penina NM, Stelmakh VF, Tolstykh VP, Zaitsev AM, The 7th Int.Conf.IBMM 90, Abstracts, Knoxville, USA. 1990;313.

[14] Efimov VG, Erchak DP, Gelfand RB, Penina NM, Stelmakh VF, Varichenko VS, Ulyashin AG, Zaitsev AM. E-MRS 1990 Fall Meeting, Abstracts, Strasbourg, France, 1990, p.C-V/P 12.

[15] Kawabata K, Mizutani M, Fukuda M, Mizogami S. Ferromagnetism of Pyrolytic Carbon under Low-Temperature Growth by the CVD Method, Synthetic Metals. 1989;33:399-402.

[16] Erchak DP, Efimov VG, Zaitsev AM, Stelmakh VF, Penina NM, Varichenko VS, Tolstykh VP. Peculiarities of Damage in Diamond Irradiated by High Energy Ions. Nucl. Instrum. Meth. in Phys. Res. B. 1992;69:443-451.

[17] Erchak DP, Guseva MB, Alexandrov AF, Alexander H, Pilar v, Pilchau A, Pis'ma Zh. Experiment. Teor. Fiz. 1993;58(N4):268-271. JETP Letters, Spin Waves in Boron Implanted Polycrystalline Diamond Films. 1993;58(N4):275-278.

[18] Ertchak DP, Efimov VG, Stelmakh VF, Review Zh. Prikladn. Spectr. 1997;64(N4): 421-449. ESR-Spectroscopy of Low Dimension Structures Produced in Natural Diamonds and Synthetic Diamond Films by Ion Implantation. J. Appl. Spectr. 1997;64(N 4):433-460.

[19] Ertchak DP, Efimov VG, Stelmakh VF, Martinovich VA, Alexandrov AF, Guseva MB, Penina NM, Karpovich IA, Varichenko VS, Zaitsev AM, Fahrner WR, Fink D. The Origin of Dominating ESR-Absorption in Ion Implanted Diamonds. Phys. Stat. Sol. B. 1997;203(N2) 529-548

[20] Dmitri Yerchuck, Alla Dovlatova. Quantum Optics Effects in Quasi-One-Dimensional and Two-Dimensional Carbon Materials. J. Phys. Chem. C. DOI: 10.1021/jp205549b. 2012;116(N1):63-80.

[21] Yearchuck D, Yerchak Y, Alexandrov A. Antiferroelectric Spin Wave Resonance. Phys. Lett. A. 2009;373(N4):489-495.

[22] Alla Dovlatova, Dmitry Yearchuck. QED Model of Resonance Phenomena in Quasionedimensional Multichain Qubit Systems. Chem. Phys. Lett. 2011;511:151-155.

[23] Dmitri Yerchuck, Alla Dovlatova, Yauhen Yerchak, Vyacheslav Stelmakh, Andrey Alexandrov, in press.

[24] Bardeen J, Cooper LN, Schrieffer JR, Microscopic Theory of Superconductivity. Phys. Rev., Letters to the Editor. 1957;108:162-164.

[25] Bardeen J, Cooper LN, Schrieffer JR, Theory of Superconductivity. Phys. Rev. 1957;108(N5):1175-1204.

[26] Dyson FD. Electron Spin Resonance Absorption in Metals. II.Theory of Electron Diffusion and the Skin Effect, *Phys. Rev.*. 1955;98(N2):349-359.

[27] Erchak DP, Zaitsev AM, Stel'makh VF, Tkachev VD, Phys. Tekhn. Polupr. Electron Spin Resonance in p-i-n Silicon Structures. 1980;14(N1):139-143. Sov. Phys. Semicond. USA. 1980;14(N1):79-82.

[28] Poole CP Jr. Technique of EPR-spectroscopy, Moscow, Mir. 1970;557.

[29] Sin-itiro Tomonaga. Remarks on Bloch's Method of Sound Waves Applied to Many-Fermion Problems. Prog. Theor. Phys. 1950;5(N4):544-569.

[30] Luttinger JM. An Exactly Soluble Model of a Many-Fermion System. J. Math. Phys. 1963;4:1154.

[31] Haldane FDM. 'Luttinger Liquid Theory' of One-Dimensional Quantum Fluids. I. Properties of the Luttinger Model and their Extension to the General 1D Interacting Spinless Fermi Gas, J. Phys. C: Solid State Physics. 1981;14:2585. DOI:10.1088/0022-3719/14/19/010

[32] Haldane FDM. Luttinger Theorem and Bosonization of the Fermi Surface, Proceedings of the International School of Physics "Enrico Fermi", Course CXXI:"Perspectives in Many-Particle Physics", eds. Broglia R and Schrieffer J.R, North Holland, Amsterdam. 1994;5-30.

[33] Pellegrino FMD, Angilella GGN, Pucci R, Ballistic Transport Properties across Nonuniform Strain Barriers in Graphene, High Pressure Research: An International Journal. 2012;32(N1):18-22. DOI:10.1080/08957959.2011.653686

[34] Rosenau da Costa M, Shelykh IA, Bagraev NT, Fractional Quantization of Ballistic Conductance in 1d Hole Systems. Phys. Rev. B. DOI: 10.1103/PhysRevB.76.201302

[35] Alla Dovlatova, Dmitri Yerchuck, Felix Borovik. Quantum Fermi Liquid Decription of (Quasi)-One-Dimensional Electronic Systems. arXiv:1112.3339 [cond-mat.str-el]

[36] Su WP, Schrieffer JR, Heeger AJ. Solitons in Polyacetylene. Phys. Rev. Lett. 1979;42:1698-1701.

[37] Su WP, Schrieffer JR, Heeger AJ. Soliton Excitations in Polyacetylene, Phys. Rev. B. 1980;22:2099-2111.

[38] Lifshitz EM, Pitaevsky LP. Statistical Physics, part 2, M., Nauka. 1978;448.

[39] Heeger AJ, Kivelson S, Schrieffer JR, Su WP. Solitons in Conducting Polymers. Rev. Mod. Phys. 1988;60:781-850.

[40] Kittel C. Theory of Antiferromagnetic Resonance. Phys. Rev. 1951;82:565.

[41] Dmitri Yerchuck, Yauhen Yerchak, Vyacheslav Stelmakh, Alla Dovlatova, Andrey Alexandrov. Ferrimagnetic Spin-Wave Resonance and Superconductivity in Carbon Nanotubes Incorporated in Diamond Matrix. J. Supercond. Nov. Magn. DOI 10.1007/s10948-013-2300-7

[42] Zhang J, Sknepnek R, Schmalian J, Phys. Rev. B. 2010;82:134527.

[43] Korshunov MM, Eremin I. Phys. Rev. B. 2008;78:140509(R).

[44] Rao SS, Stesmans A, Noyen JV, Jacobs P, Sels B. ESR Evidence for Disordered Magnetic Phase from Ultra-Small Carbon Nanotubes Embedded in Zeolite Nanochannels. Europhys. Lett. 2010;90(N5):57003.

[45] Wallace PR. The Band Theory of Graphite. Phys. Rev. 1947;71:622-634.

[46] Castro Neto AH, Guinea F, Peres NMR, Novoselov KS, Geim AK, The Electronic Properties of Graphene. Rev. Mod. Phys. 2009;81:109-162.

[47] Shaltiel D, Krug von Nidda HA, Shapiro BYa, Loidl A, Tamegai T, Kurz T, Bogoslavsky B, Rosenstein B, Shapiro I. Investigating Superconductivity with Electron Paramagnetic Resonance (EPR) Spectrometer, In: Superconductors - Properties, Technology, and Applications. Yury Grigorashvili (Ed.), In Tech. 2012;436.

[48] Hidekazu Mukuda, Mariko Nitta, Mitsuharu Yashima, Yoshio Kitaoka, Parasharam M. Shirage, Hiroshi Eisaki, and Akira Iyo, Coherence Effect of Sign-Reversing $s^{+}$-Wave Cooper Pair State in Heavily Overdoped LaFeAsO-based Superconductor: 75As-Nuclear Quadrupole Resonance. J. Phys. Soc. Jpn. 2010;79(N11):113701/1-4. DOI:10.1143/JPSJ.79.113701

[49] Alla Dovlatova, Dmitri Yerchuck. Quantum Field Theory of Dynamics of Spectroscopic Transitions by Strong Dipole-Photon and Dipole-Phonon Coupling, International Scholarly Research Network, ISRN Optics, 2012, Article ID 390749, 10 pages, DOI:10.5402/2012/390749.

[50] Dmitry Yearchuck, Yauhen Yerchak, Alla Dovlatova. Quantum-mechanical and Quantum-electrodynamic Equations for Spectroscopic Transitions. Optics Communications. 2010;283:3448-3458.

[51] Tavis M, Cummings FW. Exact Solution for an N-Molecule-Radiation-Field Hamiltonian. Phys. Rev. 1968;170(2):379-384.

[52] Yearchuck D, Yerchak Y, Red'kov V. Quantum Mechanical Analogue of Landau-Lifshitz Equation. Doklady NANB. 2007;51:57-64.

[53] Leggett AJ, Chakravarty S, Dorsey AT, Fisher MP, Garg AA, Zwerger W. Dynamics of the Dissipative Two-State System. Rev. Mod. Phys. 1987;59:1-85.

[54] Mahan GD. Many-Particle Physics, Plenum, New York; 2000.

[55] Heitz R, Mukhametzhanov I, Stier O, Madhukar A, Bimberg D. Enhanced Polar Exciton-LO-Phonon Interaction in Quantum Dots. Phys. Rev. Lett. 1999;83:4654-4657.

[56] Tü rck V, Rodt S, Stier O, Heitz R, Engelhardt R, Pohl UW, Bimberg D, Steingruber R. Effect of Random Field Fluctuations on Excitonic Transitions of Individual CdSe Quantum Dots. Phys. Rev. B. 2000;61:9944.

[57] Besombes L, Kheng K, Marsal L, Mariette H. Acoustic Phonon Broadening Mechanism in Single Quantum Dot Emission. Phys. Rev. B. 2001;63:155307-5.

[58] Wilson-Rae I, Imamoglu A. Quantum Dot Cavity-QED in the Presence of Strong Electron-Phonon Interactions. Phys. Rev. B. 2002;65:23531.

[59] Ka-Di Zhu, Zhuo-Jie Wu, Xiao-Zhong Yuan, Hang Zheng. Excitonic Dynamics in a Single Quantum Dot within a Microcavity. Phys. Rev. B. 2005;71:235312.

[60] Seavey MH Jr, Tannenwald PE. Direct Observation of Spin-Wave Resonance. Phys. Rev. Lett. 1958;1(N5):168-170.

[61] Ertchak DP, Kudryavtsev YuP, Guseva MB, Alexandrov AF, Evsyukov SE, Babaev VG, Krechko LM, Koksharov YuA, Tikhonov AN, Blumenfeld LA, v.Bardeleben HJ. Electron Spin Resonance and Microwave Photoconductivity in Carbynoid Films. J. Physics: Condensed Matter. 1999;11(N3);855-870.

[62] Shaltiel D. J. Supercond. Nov. Magn. 2013;26:3005-3008. DOI 10.1007/s10948-013-2337-7.



***Peer-review history:***
*The peer review history for this paper can be accessed here (Please copy paste the total link in your browser address bar)*
*www.sciencedomain.org/review-history.php?iid=482&id=22&aid=4169*